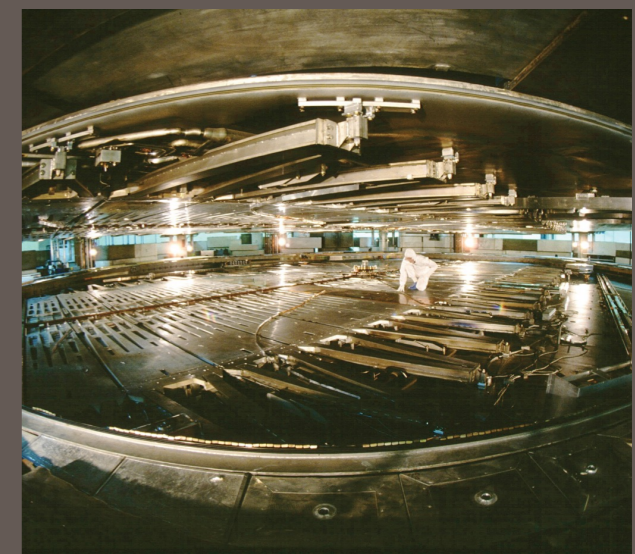


Commissioning of and First Measurements with TRIUMF's ElectroMagnetic Mass Analyser (EMMA)

June 18th, 2018

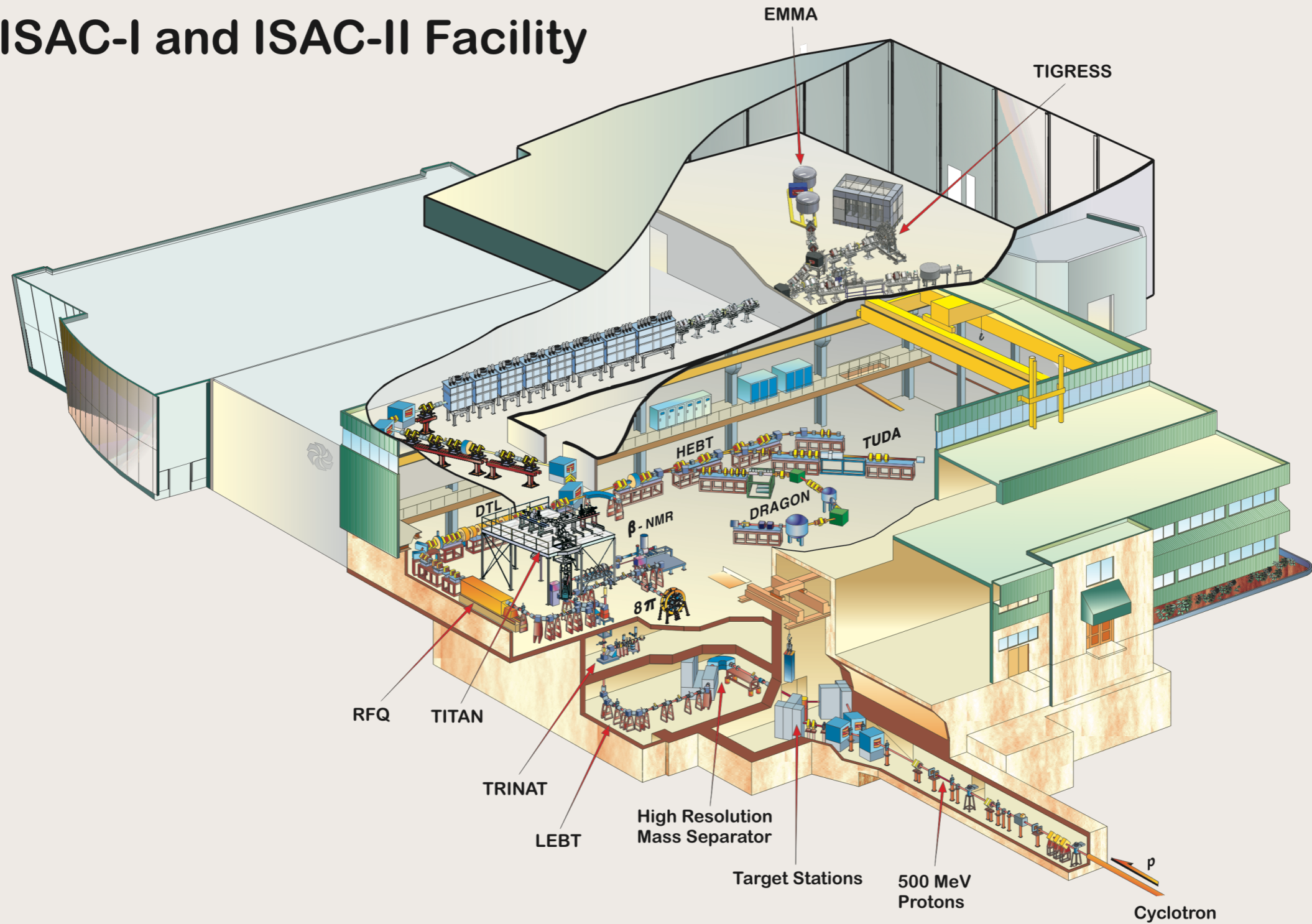
Barry Davids

TRIUMF & Simon Fraser University



EMMA in ISAC-II

ISAC-I and ISAC-II Facility



Nuclear Structure at the Extremes

- Single-particle structure at extreme N/Z values, particularly at and near closed shells (single-nucleon transfer)
- Pairing interactions in $N \sim Z$ nuclei via (p,t) , $({}^3\text{He},p)$, (d,α) , (t,p)
- Production and decay studies of highly neutron-rich nuclei via multi-neutron transfers, e.g. $({}^{18}\text{O},{}^{15}\text{O})$
- High-spin physics in neutron-deficient nuclei via fusion-evaporation reactions (including isomers)

Nuclear Astrophysics

- Direct Studies:
 - Radiative capture reactions
 - (α, n) and (α, p) reactions
 - Time-reversed (α, p) reactions
- Indirect Studies:
 - Spectroscopy of unbound states
 - Particle-decay branching ratios



Defining the Problem I

- In transfer and fusion-evaporation reactions, spectroscopic information obtained from detecting light ejectiles and gamma rays
- Interpretation of spectra complicated or rendered impossible by background from other channels
- For transfers with light ejectile detection, kinematic lines obscured by diffuse background
- For fusion-evaporation, gamma spectra contaminated by lines from other nuclei, frequently produced much more copiously than the nucleus of interest
- Direct identification of residual nuclei required

Defining the Problem II

- Use of particle detectors to directly detect recoils complicated by 2 problems:
 - In both fusion-evaporation and transfer reactions in inverse kinematics, heavy recoils emerge from target within the cone of elastically scattered beam particles; for sufficiently intense beams, these detectors cannot count fast enough
 - For heavy recoils ($m > 100$ u), energy resolution of these detectors is insufficient to permit unique identification
- Recoil separator needed to separate recoils from beam, identify according to A and Z, and localize them for subsequent decay studies

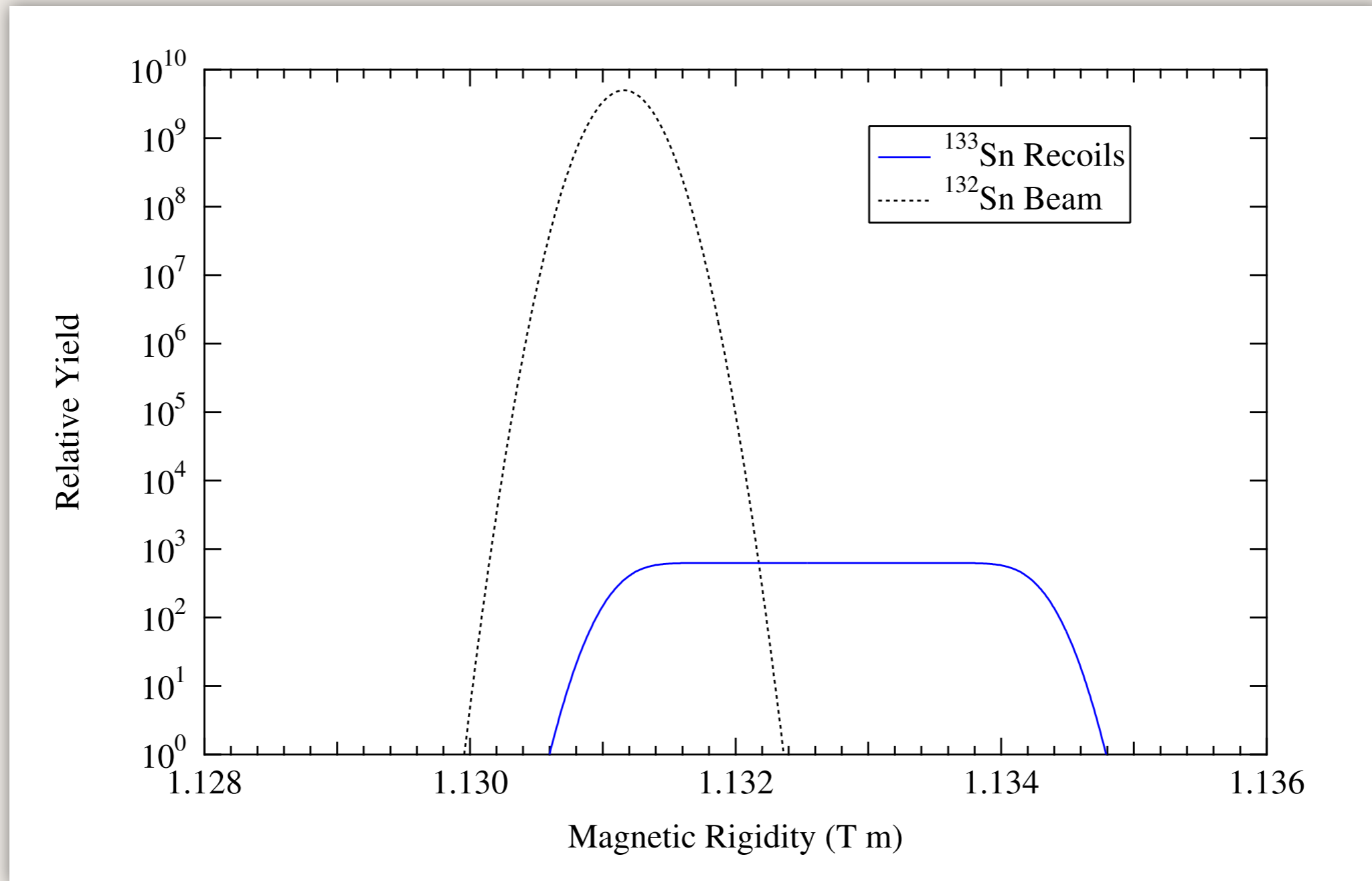
Requirements

- Must be capable of 0° operation with good beam rejection
- Short flight time will allow study of short half-life radioactivities
- Good energy resolution is not helpful
 - Energy and angular resolution of detected heavy recoils insufficient to resolve states for $A > 30$ beams
 - Energy-focussing operation desirable
- Large angular, mass/charge, and energy acceptances required for high collection efficiency
 - Angular acceptance should be symmetric
 - At least 2 charge states for sufficiently massive recoils

Acceptance and Resolution

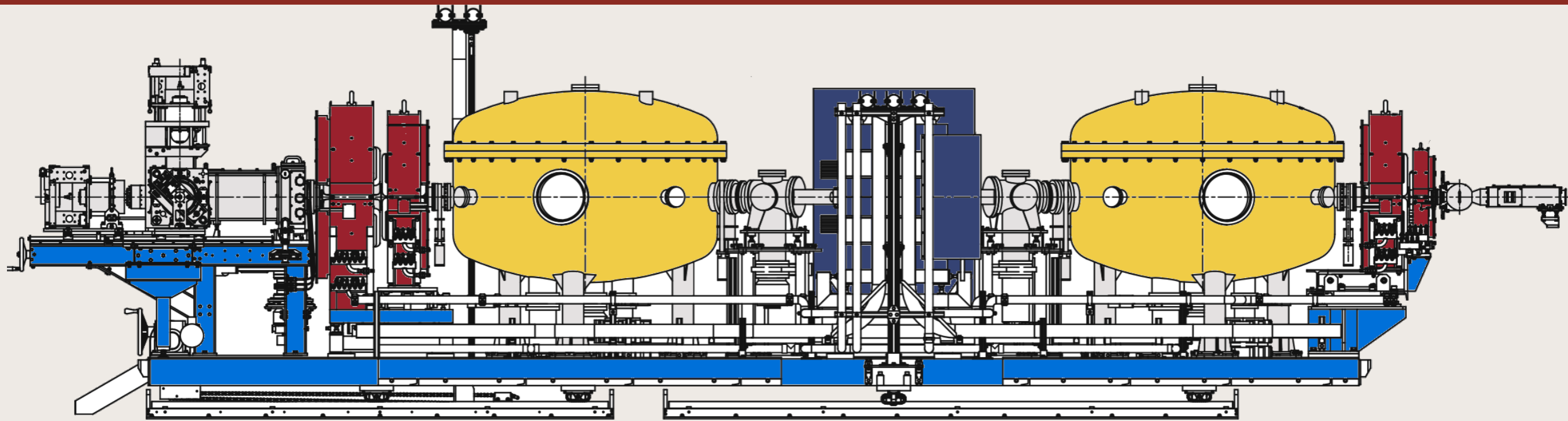
- Angular and energy spreads largest for fusion-evaporation reactions ($\Omega \sim 10\text{-}30$ msr, $\Delta E/E \sim \pm 20\%$)
- Angle and energy spread not independent
- To take advantage of large angular acceptance, need large energy acceptance
- Large energy acceptance requires minimal chromatic aberrations to maintain resolving power
- Mass resolution requirement set by single-nucleon transfer reactions in inverse kinematics: must have first order resolving power $M/\Delta M \geq 400$

How About a Magnetic Spectrometer?



$d(^{132}\text{Sn}, p)^{133}\text{Sn}$ at 6 A MeV with $100 \mu\text{g cm}^{-2}$ $(\text{CD}_2)_n$ target; smallest achievable beam energy spread; protons from 90-170 deg in lab

EMMA: The ISAC-II Recoil Spectrometer



- EMMA: recoil mass spectrometer spatially separates heavy products of nuclear reactions from beam & disperses according to mass/charge ratios
- 4 magnetic quadrupole lenses, 1 dipole magnet, 2 electrostatic deflectors, 3 slit systems, target chamber with integral Faraday cup, and modular focal plane detection system w/ PGAC, ionization chamber, and Si detectors
- Magnets and deflectors from contractor, other components TRIUMF-built

Elementary Ion Optics I

- Reference particle with mass m_0 , charge q_0 , and momentum p_0 or kinetic energy T_0
- Ion optical coordinates: x, y

$$a = \frac{p_x}{p_0} \simeq \theta, \quad b = \frac{p_y}{p_0} \simeq \phi$$

$$\delta_m = \frac{\frac{m}{q} - \frac{m_0}{q_0}}{\frac{m_0}{q_0}}, \quad \text{and} \quad \delta_T = \frac{\frac{T}{q} - \frac{T_0}{q_0}}{\frac{T_0}{q_0}}.$$

$$x_f = x_f(x_i, y_i, a_i, b_i, \delta_m, \delta_T).$$

Elementary Ion Optics II

- Notation:

$$(x | x) \equiv \frac{\partial x_f}{\partial x_i}, \quad (x | xy) \equiv \partial_{x_i} \partial_{y_i} x_f, \quad \text{etc.}$$

$$x = \sum_{j=1}^6 r_j (x | r_j) + \frac{1}{2} \sum_{i=1}^6 \sum_{j=1}^6 r_i r_j (x | r_i r_j) + \frac{1}{6} \sum_{i=1}^6 \sum_{j=1}^6 \sum_{k=1}^6 r_i r_j r_k (x | r_i r_j r_k) + \dots$$

First Order Optics

- Mid-plane symmetry in non-dispersive direction implies terms linear in y and b vanish, so to 1st order

$$x_f = (x|x)x_i + (x|a)a_i + (x|\delta_m)\delta_m + (x|\delta_T)\delta_T.$$

- Spectrometers use quadrupoles and magnet edge angles to arrange a point-to-point angular focus:

$$(x|a) = 0, \text{ so}$$

$$x_f = (x|x)x_i + (x|\delta_m)\delta_m + (x|\delta_T)\delta_T$$

Electromagnetic Spectrometers

- Energy focussing: $(x | \delta_T) = 0$
- Hence first order equations describing recoil mass spectrometers and magnetic spectrometers have identical form:

$$x_f = (x | x)x_i + (x | \delta_m)\delta_m$$

$$x_f = (x | x)x_i + (x | \delta_p)\delta_p$$

Resolving Power

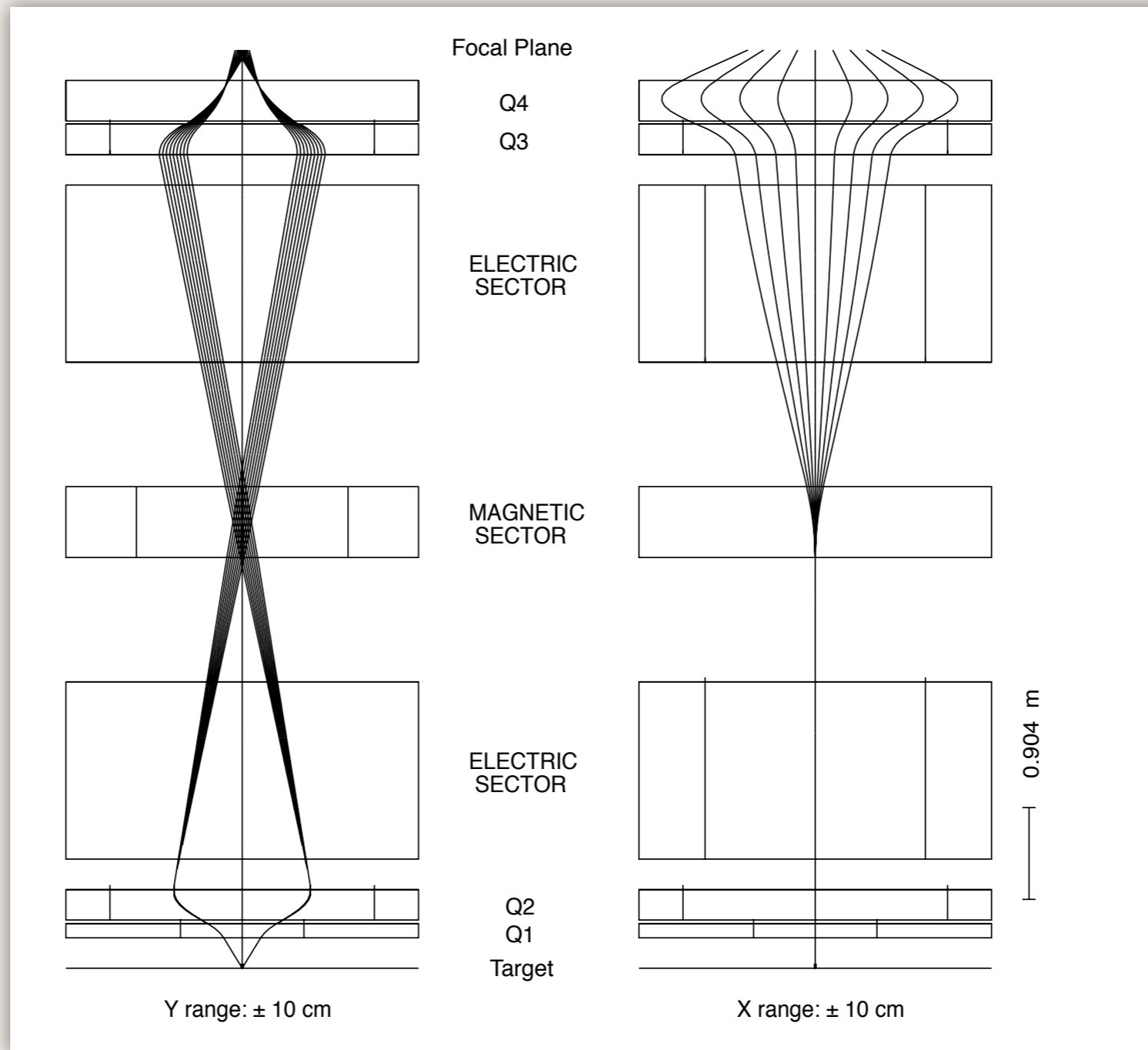
- Resolving power, first order expression:

$$R_m = \frac{m/q}{\Delta(m/q)} = \frac{(x | \delta_m)}{2(x | x)x_i} \quad \text{and} \quad R_p = \frac{p/q}{\Delta(p/q)} = \frac{(x | \delta_p)}{2(x | x)x_i}$$

- Limited by higher-order aberrations; some corrections possible
- Typical values:

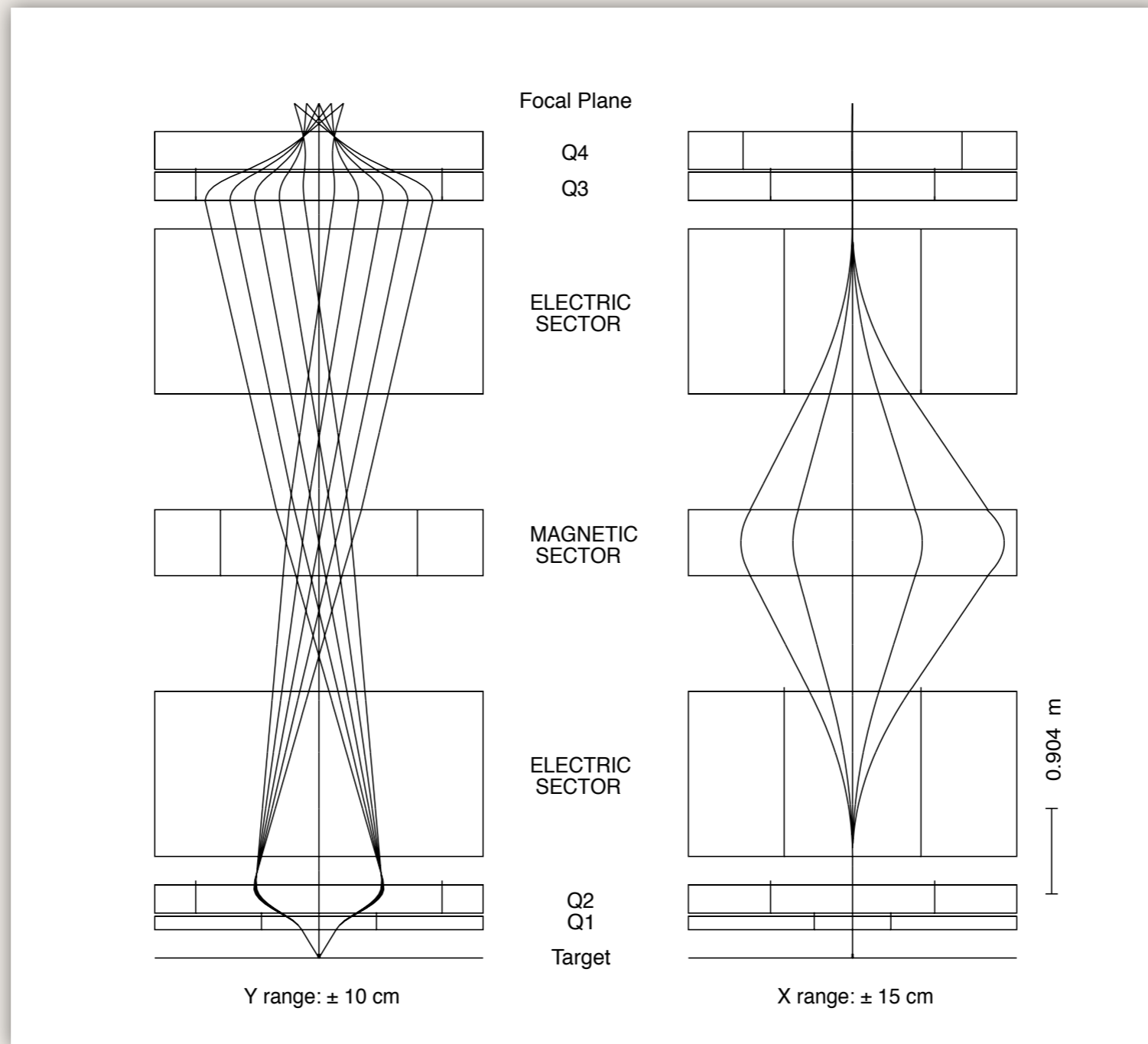
$$R_p = 1000 - 20000 \quad \text{and} \quad R_m = 100 - 600$$

EMMA Ion Optics: Spatial Focus



9 Adjacent Masses Emitted from Target with Vertical Angles
of $0, \pm 2^\circ$

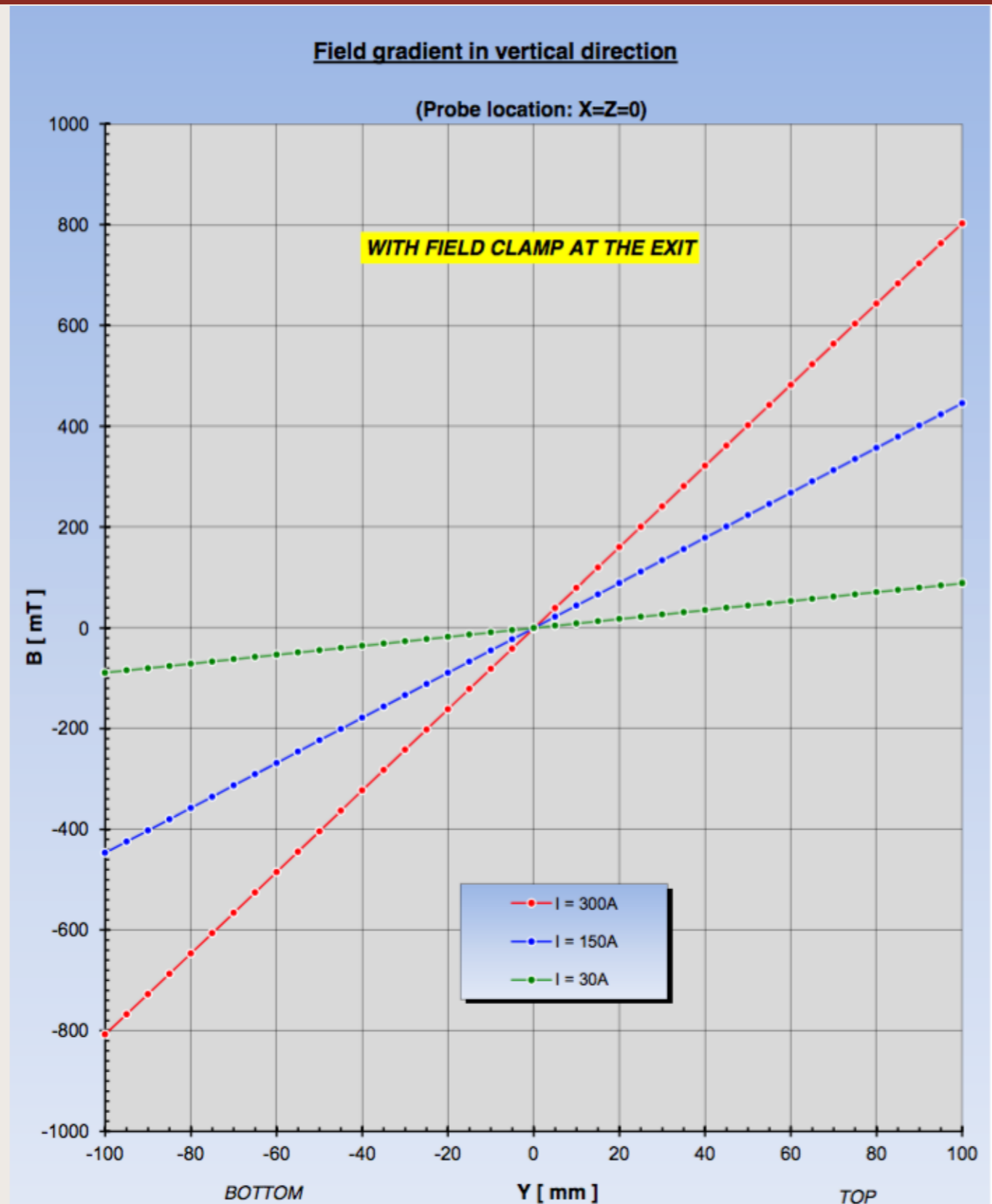
EMMA Ion Optics: Energy Focus



Single Mass, Vertical Angles of $0, \pm 2^\circ$, Energies Deviating from Central Value by $0, \pm 7.5\%$ and $\pm 15\%$

Quadrupole Tests at Manufacturer

- Various properties of 4 quadrupole magnets measured by manufacturer:
- Field Gradient
- Effective Length
- Effective Field
- Boundary Locations
- Higher Harmonic Content
- Deviation of Mechanical and Magnetic Axes



Quadrupole Tests at TRIUMF

- Field gradients of all 4 quadrupoles measured as a function of current using Hall effect magnetometer, which was calibrated using an NMR system and the uniform field of our dipole magnet
- Field is measured at all times using a reference probe, which was calibrated simultaneously

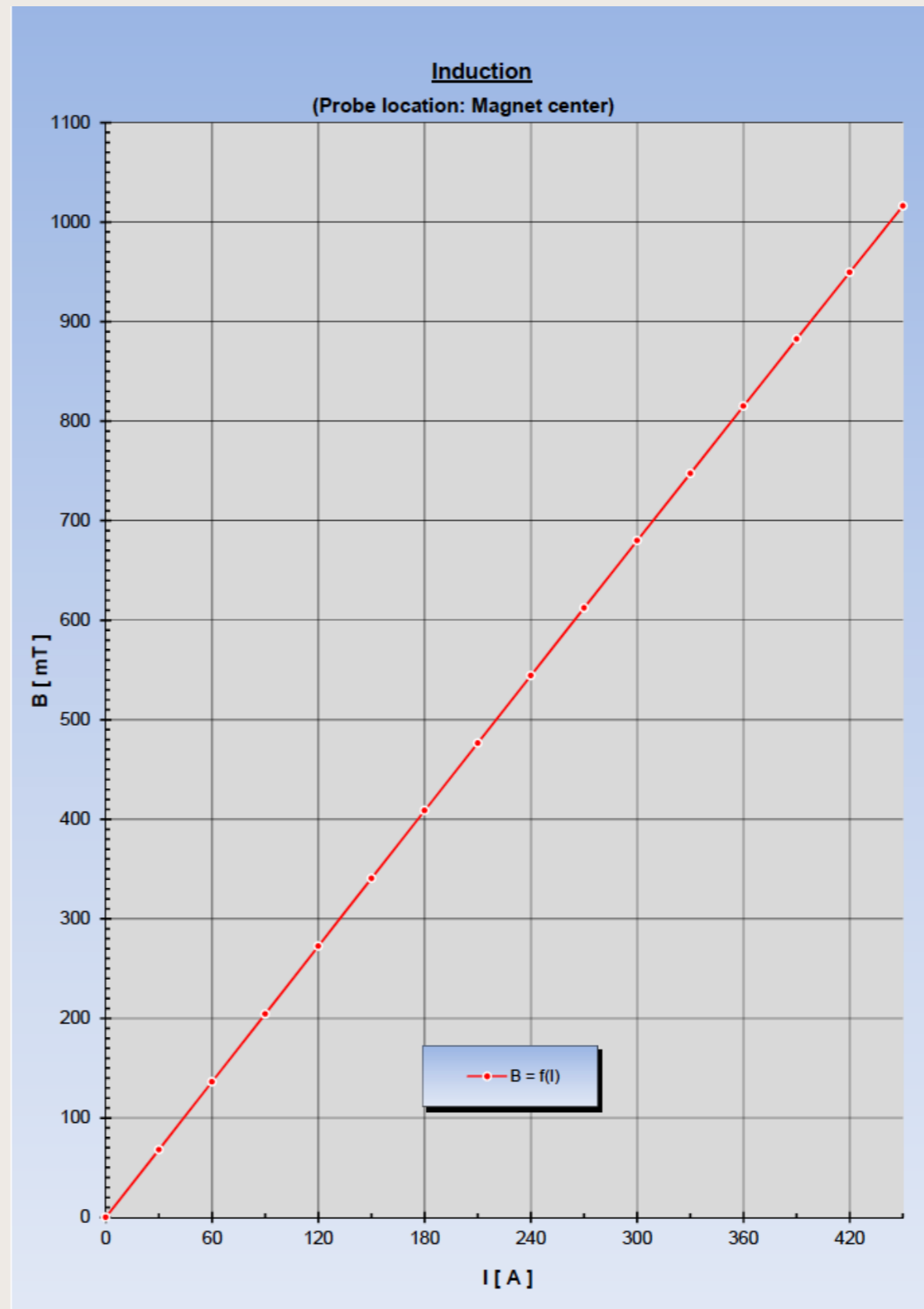


EMMA Quadrupole Lenses

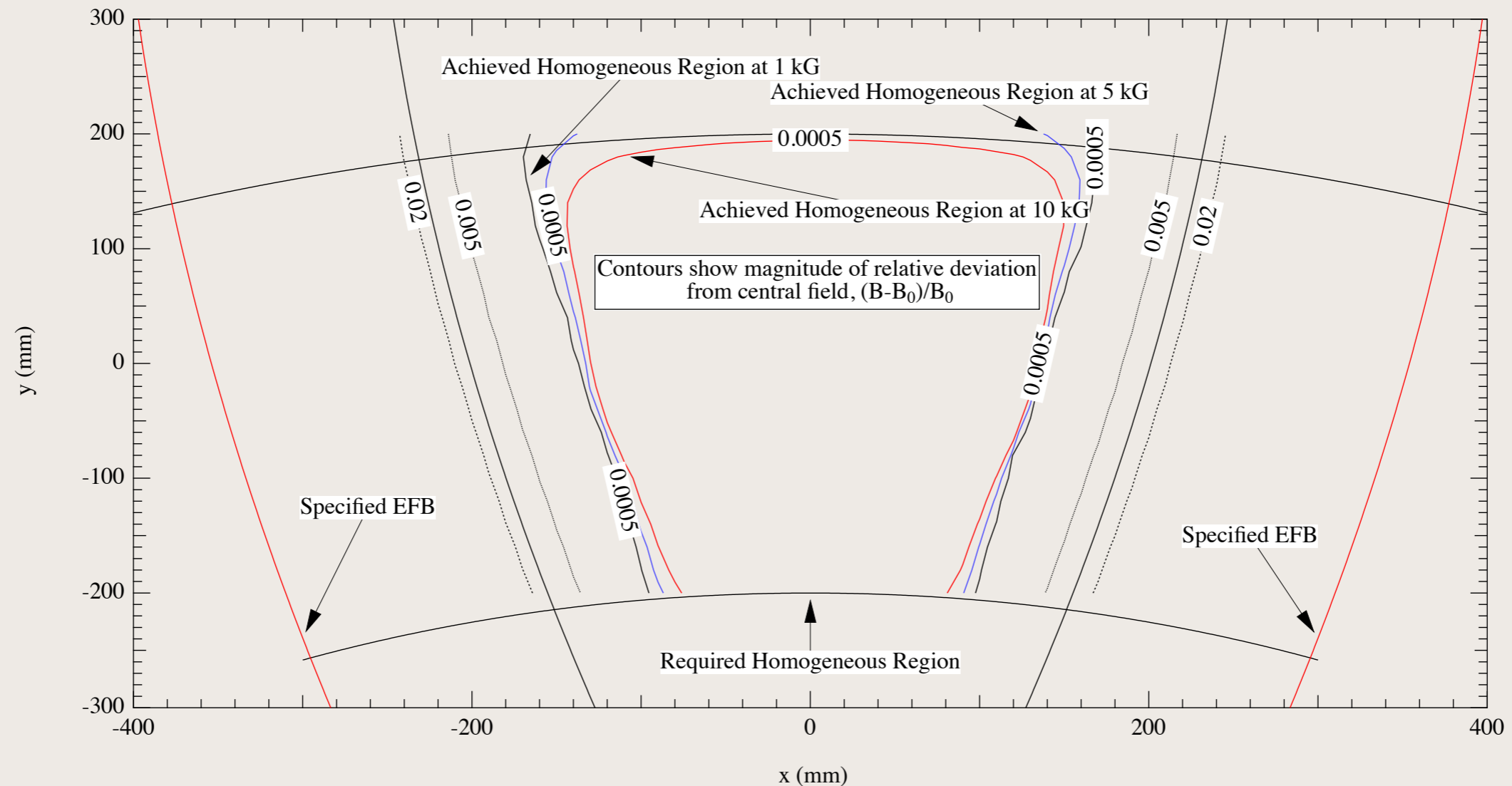
Magnetic Lenses	Quadrupole 1	Quadrupoles 2 & 3	Quadrupole 4
Bore Diameter	7 cm	15 cm	20 cm
Specified Effective Length	14 cm	30 cm	40 cm
Achieved Effective Length	13.98 cm	29.98 cm/29.88 cm	40.18 cm
Specified Maximum Pole Tip Field	1.21 T	0.87 T	0.81 T
Achieved Maximum Pole Tip Field	1.21 T	0.84 T	0.80 T
Achieved Field Gradient	34.6 T m ⁻¹	11.3 T m ⁻¹	8.4 T m ⁻¹

Dipole Tests at Manufacturer

- 40 degree dipole magnet's field mapped at manufacturer
- Removable pole shims had to be machined three times before acceptance

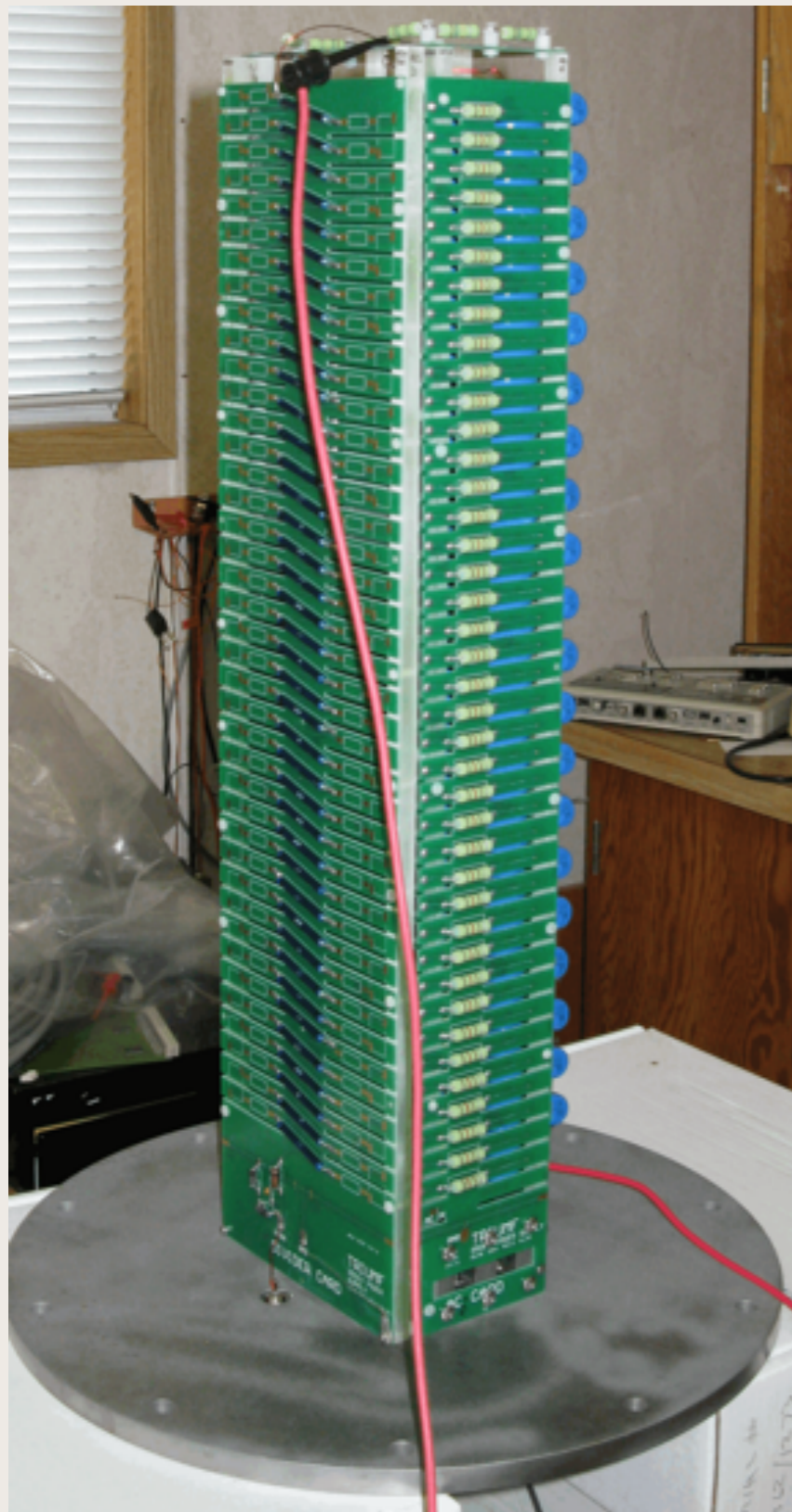


Dipole Field Map Analysis



- Homogeneity and field boundary shape at 4 different currents analyzed at TRIUMF; magnet remapped at TRIUMF
- Maximum deviation from required effective length found at bending radius of 800 mm to be just under 0.3%; on average better than 0.1%

TRIUMF-Built HV Supplies



- Built 3 positive and 3 negative
- All have been tested to $|V| \geq 325$ kV
- Housed in re-entrant ceramic vessels
- Pressurized with 3 bar SF₆

Electric Dipole, Mark I



Electrostatics

- High voltage testing at Bruker's Karlsruhe factory ended badly in 2012
- Caused by design and manufacturing flaws
- Bruker lacked appropriate HV testing space, so agreed to ship upon successful factory inspection in exchange for price reduction
- Inspection of reworked parts at Karlsruhe factory took place in Jan 2013

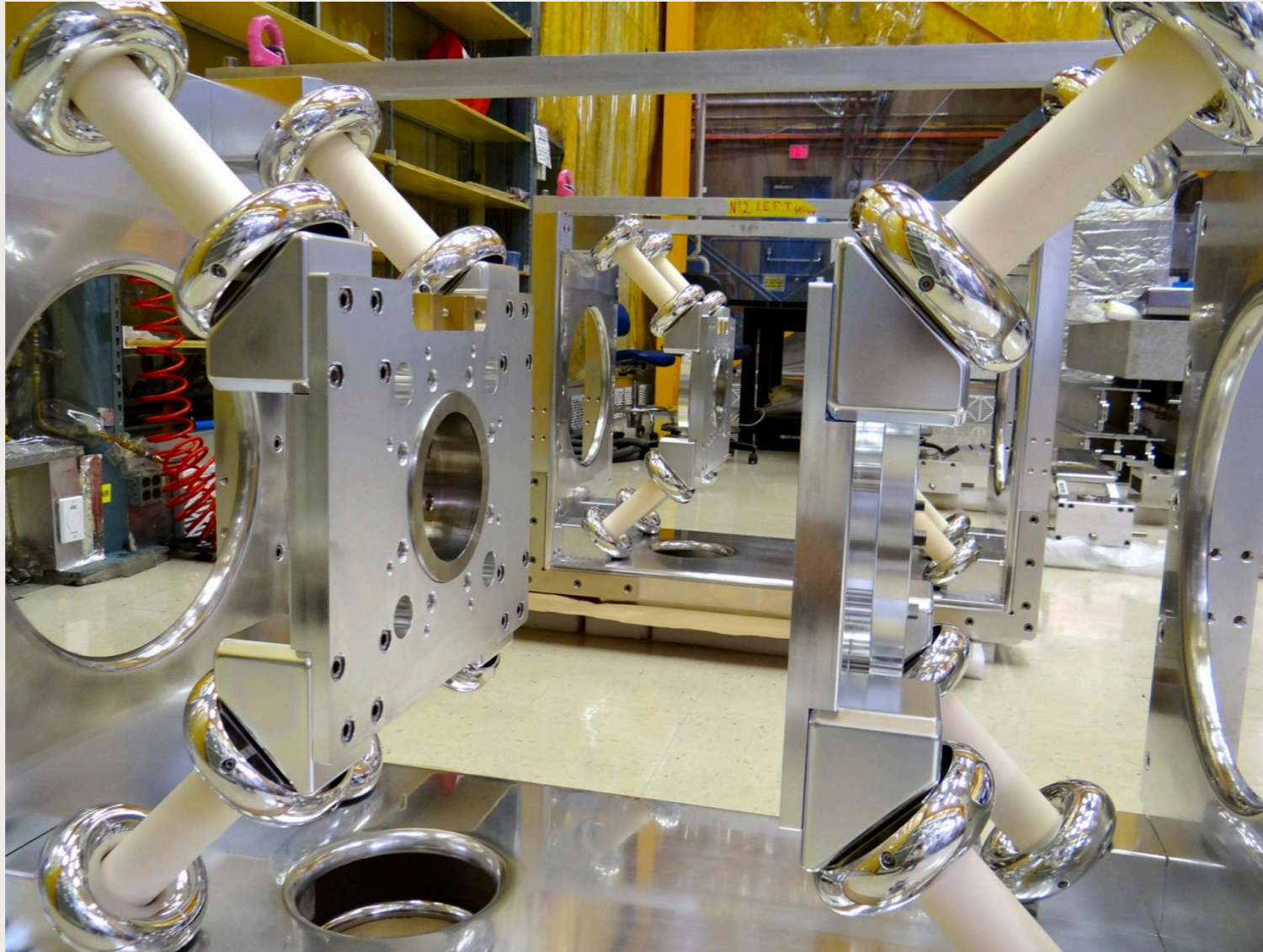
Inspection Failures

1. The new corona ring assemblies were not properly aligned.
2. There were scratches on both anodes.
3. Four rectangular electrode covers had scratches, pits, or protrusions.
4. The field clamp on the exit port of ED2 had scratches.
5. The interiors of 6 HVPS ceramic feedthroughs had gouges in their surfaces.

Electrostatics Shipment



Electrode Supports



Broken Ceramic Insulators

- 6 insulating supports arrived broken
- 4 were cracked but still intact
- 6/16 insulators had incomplete braze joints and 5 more had irregular appearances



Replacement Insulating Supports



Redesigned insulating supports arrived from Bruker in March 2015, passed load tests with no appreciable deflection

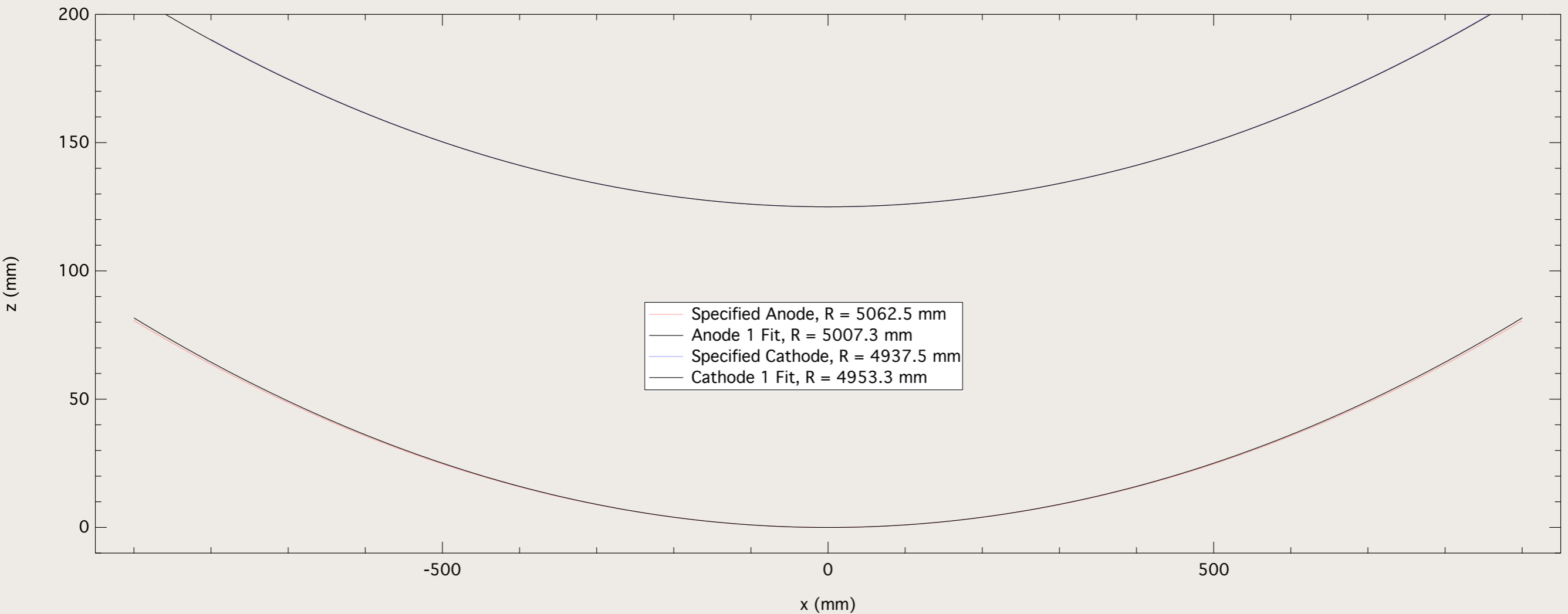
Re-polished Support Plate



Electrode Measurements

Electrode	TRIUMF R (mm)	Sicom R (mm)	Bruker R (mm)	Specified R (mm)
ED1 Anode	5007.3	4999.2	4974.5 (55)	5062.5
ED1 Cathode	4953.3	4956.0	4958.5 (55)	4937.5
ED2 Anode	4977.1		4970.8 (55)	5062.5
ED2 Cathode	4952.0		4953.3 (55)	4937.5

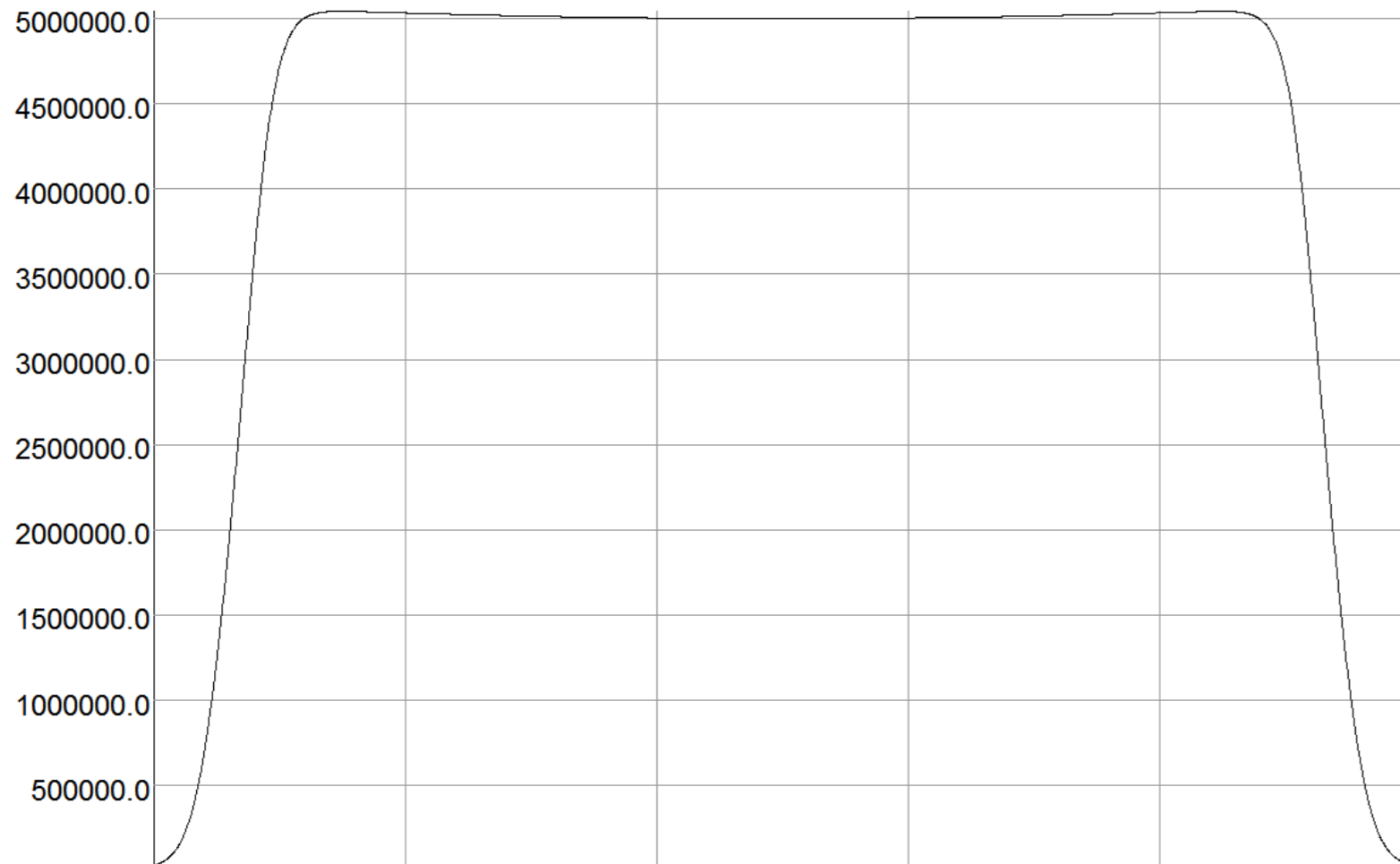
Anode Shape Problem



Aligning centres for 125 mm gap implies 124 mm gap for one pair, 123.6 mm gap for other

Finite Element Simulation

16/Nov/2015 11:01:57



X coord	-1000.652	-598.47424	-197.34652	200.135763	591.400783	973.917
Y coord	51.496	54.6196914	25.4090867	-35.946814	-129.05102	-253.301
Z coord	4.052	4.052	4.052	4.052	4.052	4.052

Component: E, from buffer: Arc, Integral = 8.7473635334383E+09

UNITS
 Length mm
 Elec Flux Density C/m²
 Electric Field V/m
 Electric Pot volt
 Power W
 Force N
 Energy J

MODEL DATA
 measured11_25-8-4.op3
 TOSCA Electrostatic
 Nonlinear materials
 Simulation No 1 of 1
 23284451 elements
 31570927 nodes
 Nodally interpolated fields
 Activated in global coordinates

Field Point Local Coordinates
 Local = Global

FIELD EVALUATIONS
 Arc ARC (nodal) 3001 Cartesian
 x=-1000.652 to 973.917 y=51.496 to -253.301 z=4.052

Opera

Effective field length is 0.25% larger due to anode radius

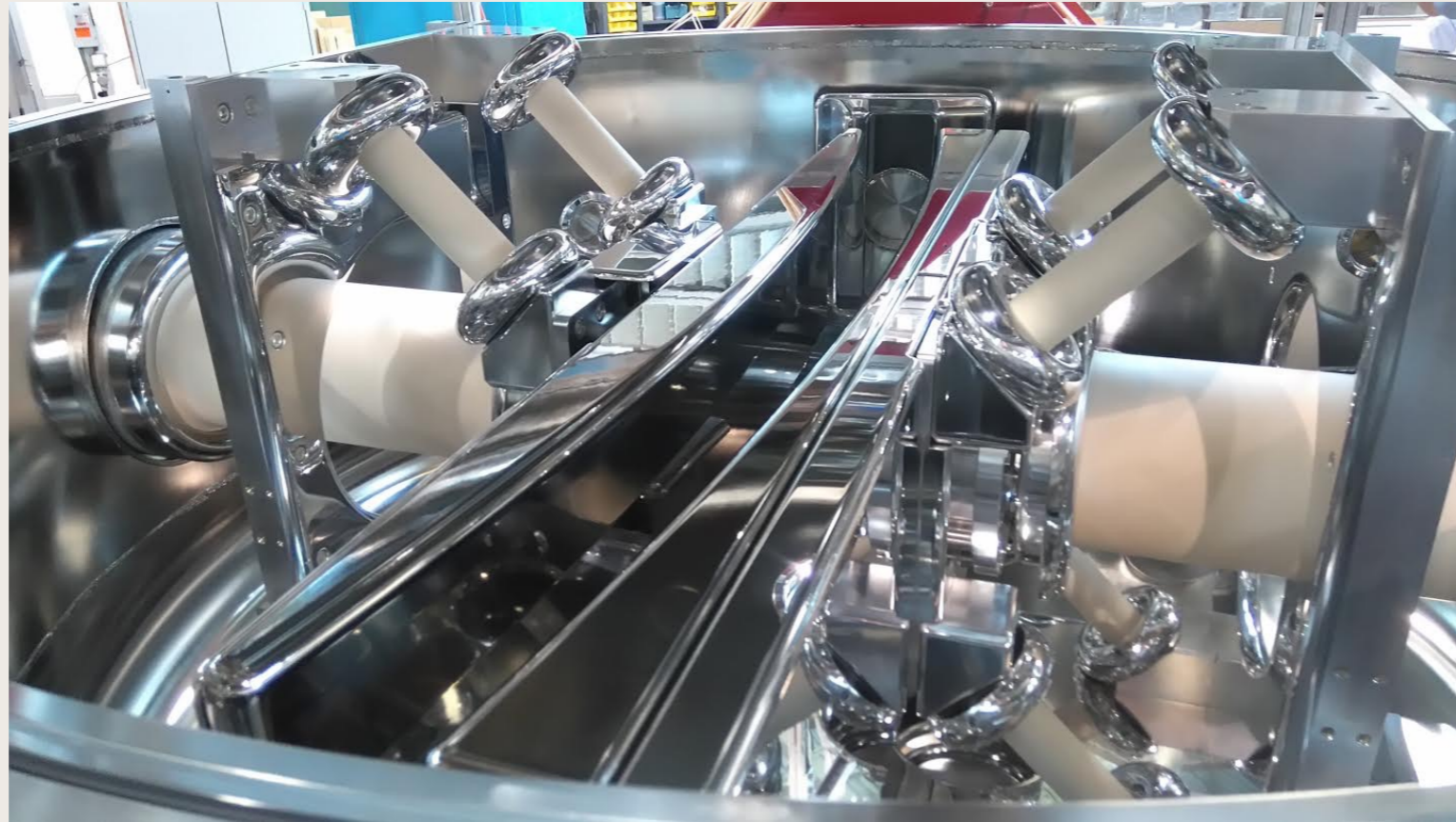
Complete ED2 Electrode



EMMA Dipoles

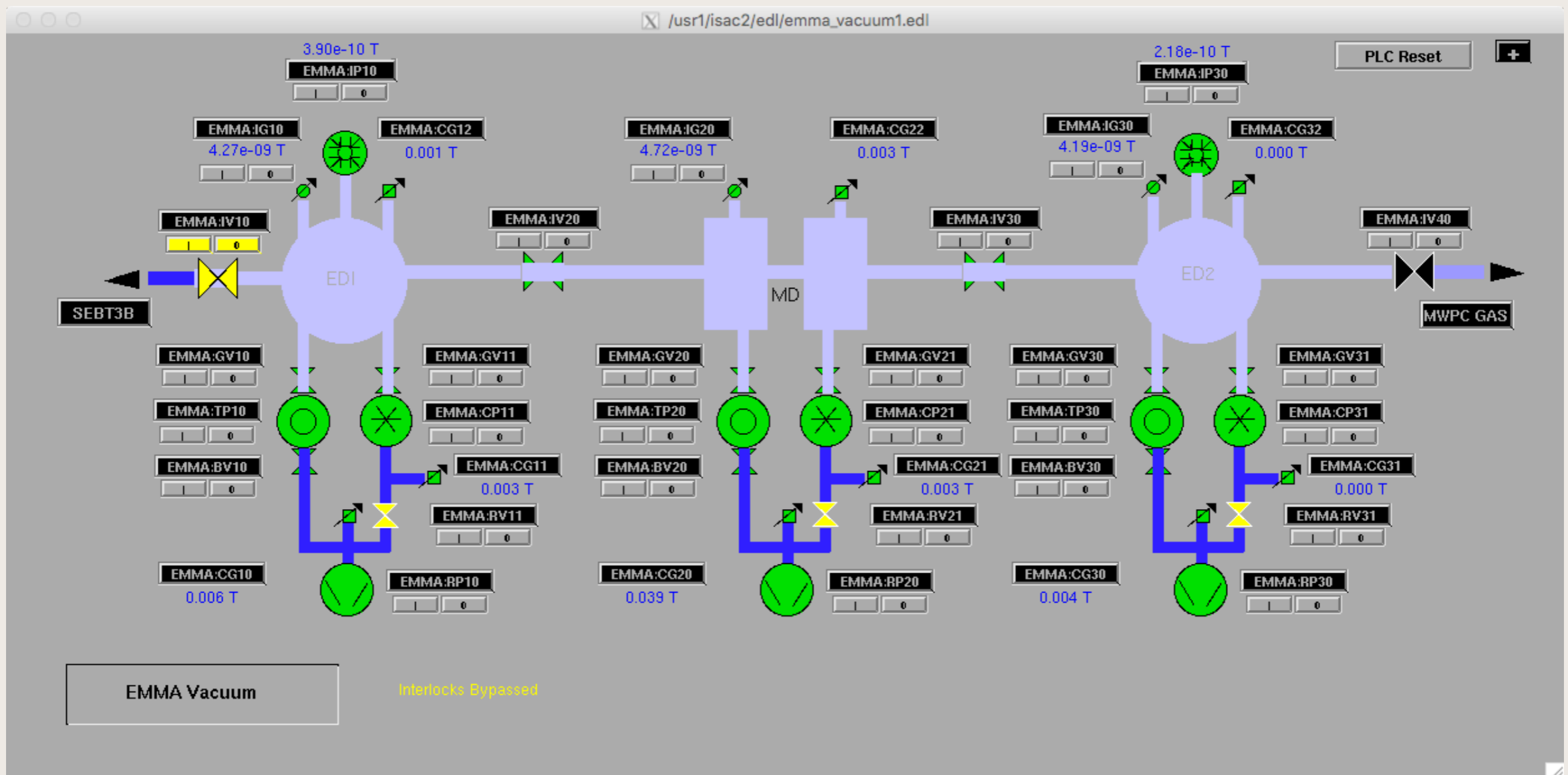
Dipoles	Magnetic	Electric
Radius of Curvature	1 m	5 m
Specified Deflection Angle	40.00°	20°
Achieved Deflection Angle	40.11°	20.05°
Specified Effective Field Boundary Inclination Angle	8.3°	0
Achieved Effective Field Boundary Inclination Angle	7.93° and 8.67°	
Effective Field Boundary Radii	3.472 m	-
Maximum Field	1 T	40 kV cm ⁻¹

HV Conditioning



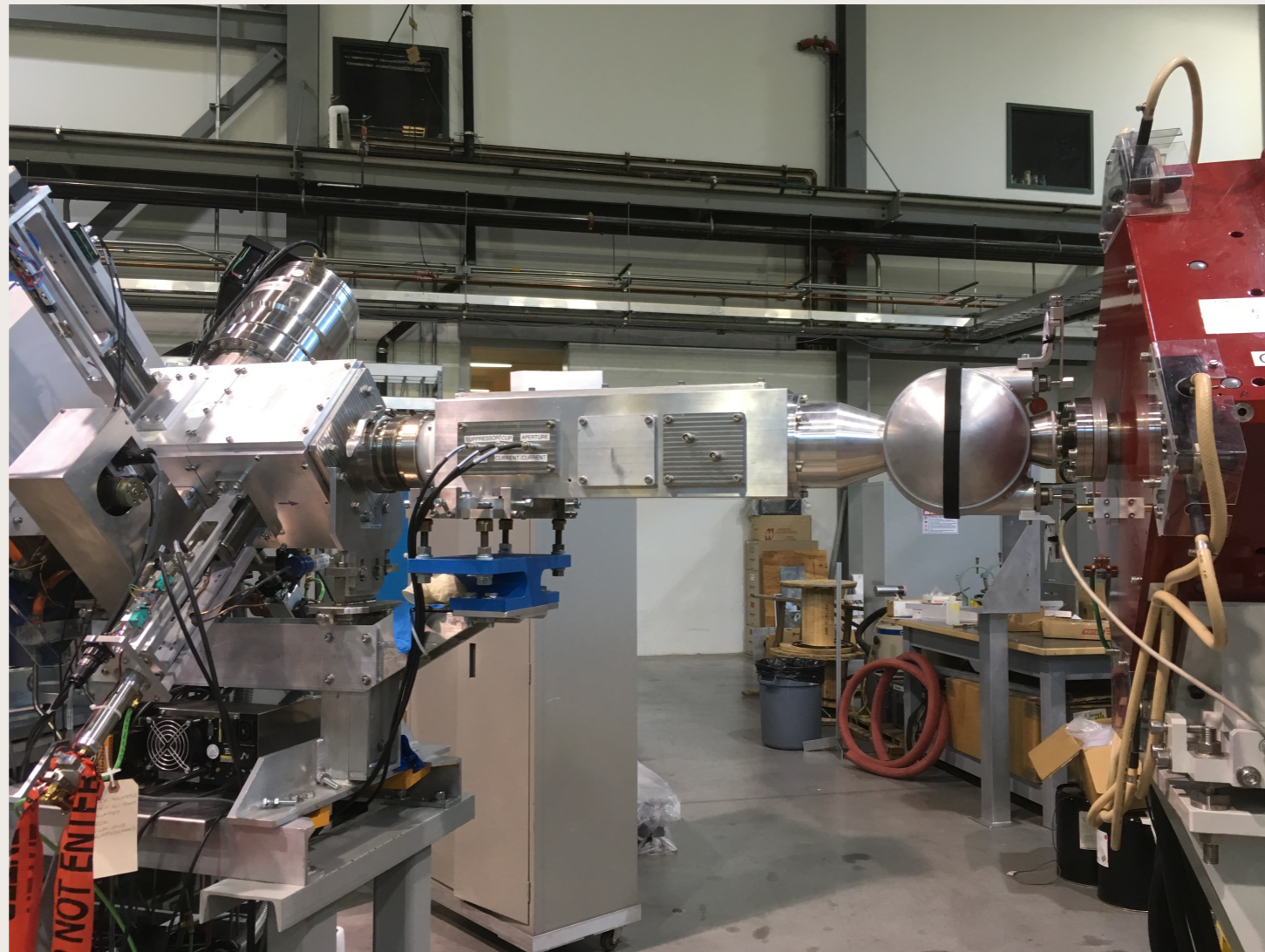
- Both anodes and cathodes conditioned alone to potential difference of 250 kV with respect to ground
- ED2 conditioned to $\Delta V = 430$ kV, ED1 has only stably reached $\Delta V = 340$ kV so far; after cleaning, noticed that electrostatic shield had rotated, exposing sharp bolts

Vacuum Systems



- Typical pressures in 3/4 vacuum sections in nTorr range; 1000 l/s turbos and 1500 l/s cryos
- Focal plane box has a single 1000 l/s turbo; pressure in 10^{-7} Torr range

Target Chamber I



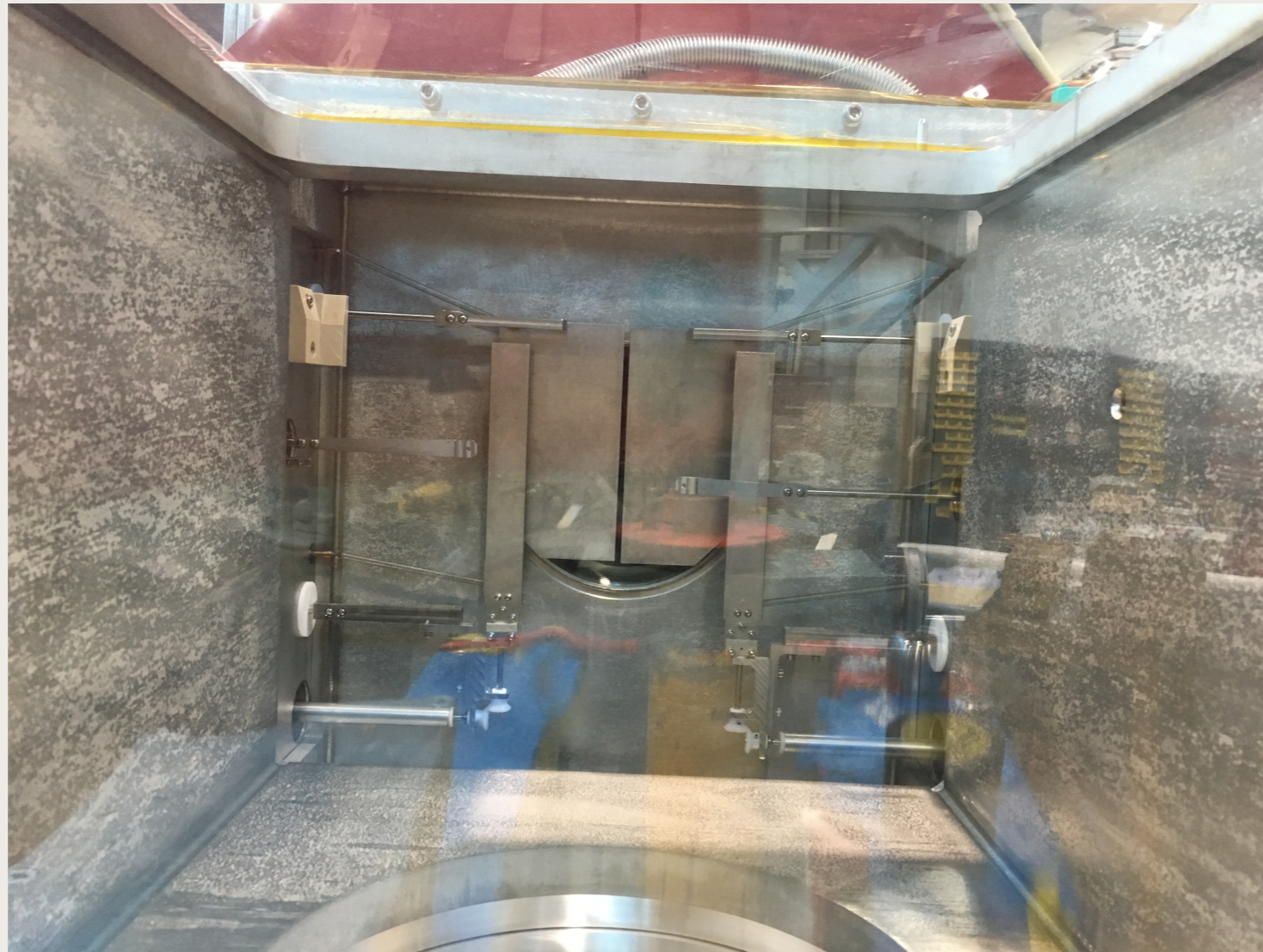
- Designed to accommodate 12/16 TIGRESS HPGe gamma-ray detectors
- Pumped by beam line 500 l/s turbo; pressure in low 10^{-7} Torr range

Target Chamber II

- Integral Faraday cup with 1 mm entrance aperture coincides spatially with target position
- Target fan with 3 positions
- Mounts for 2 Si surface barrier detectors downstream
- Upstream and downstream mounts for annular DSSDs of the S2 variety

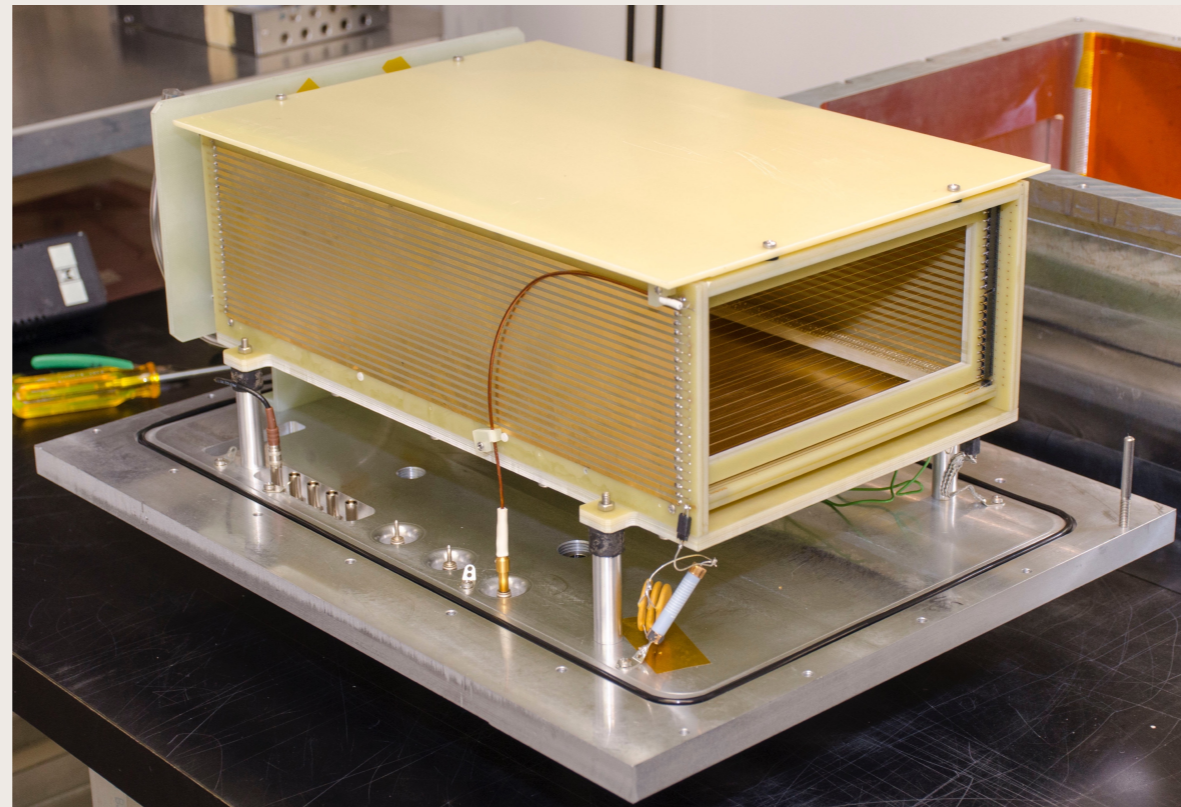
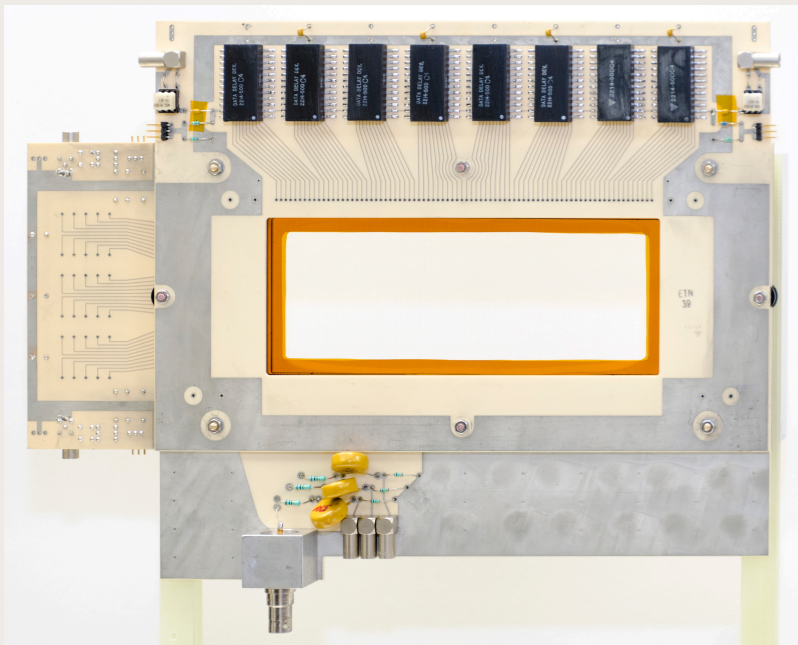


Slit Systems



- Plate slit systems upstream and downstream of dipole magnet
- More complex focal plane slit system has 2 plates and 2 rotatable fingers, allowing for 3 openings of variable width and position

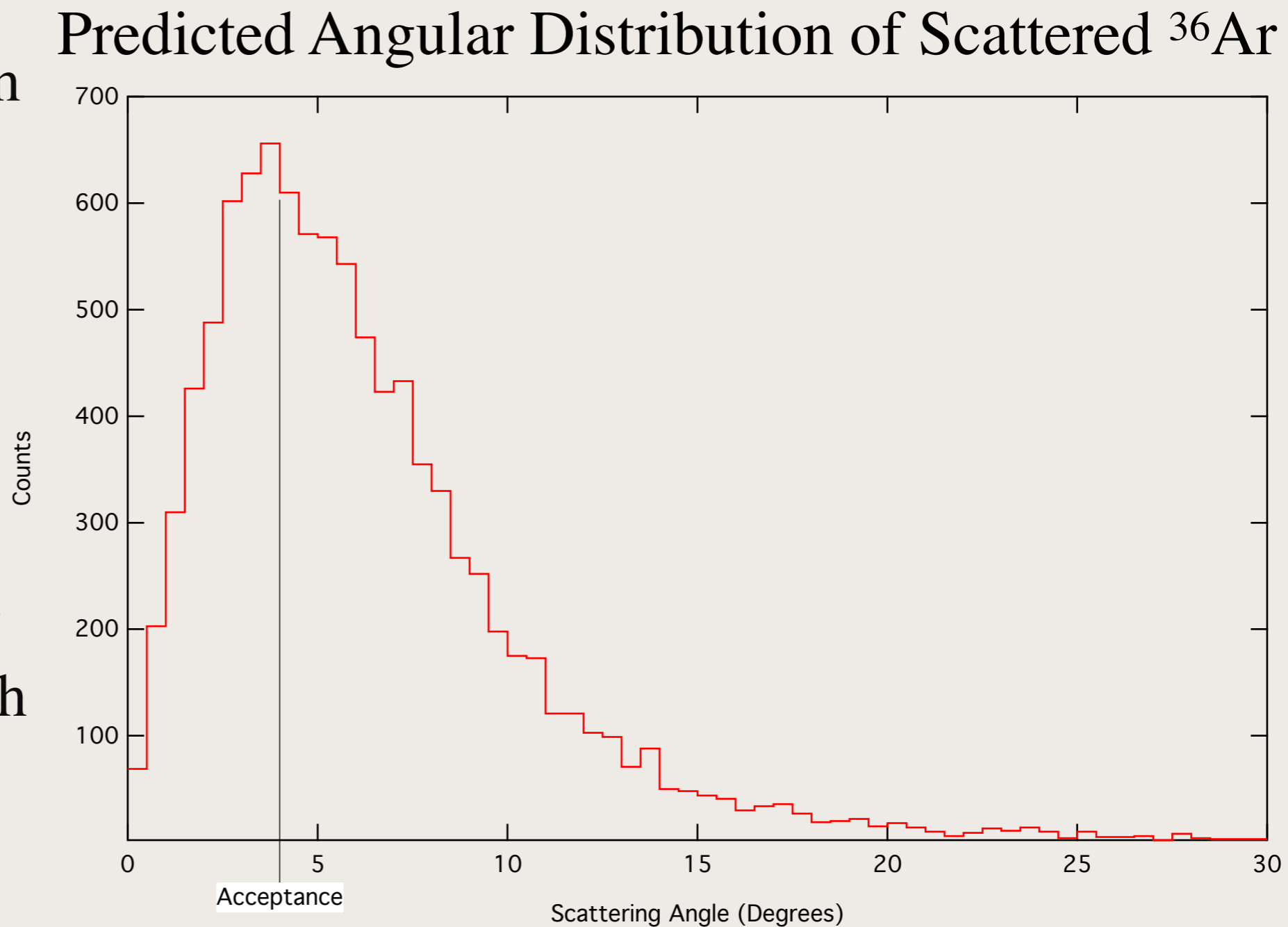
Focal Plane Detectors



- PGAC measures position (m/q), energy loss
- Ionisation chamber measures energy losses
- Si detector measures residual energy

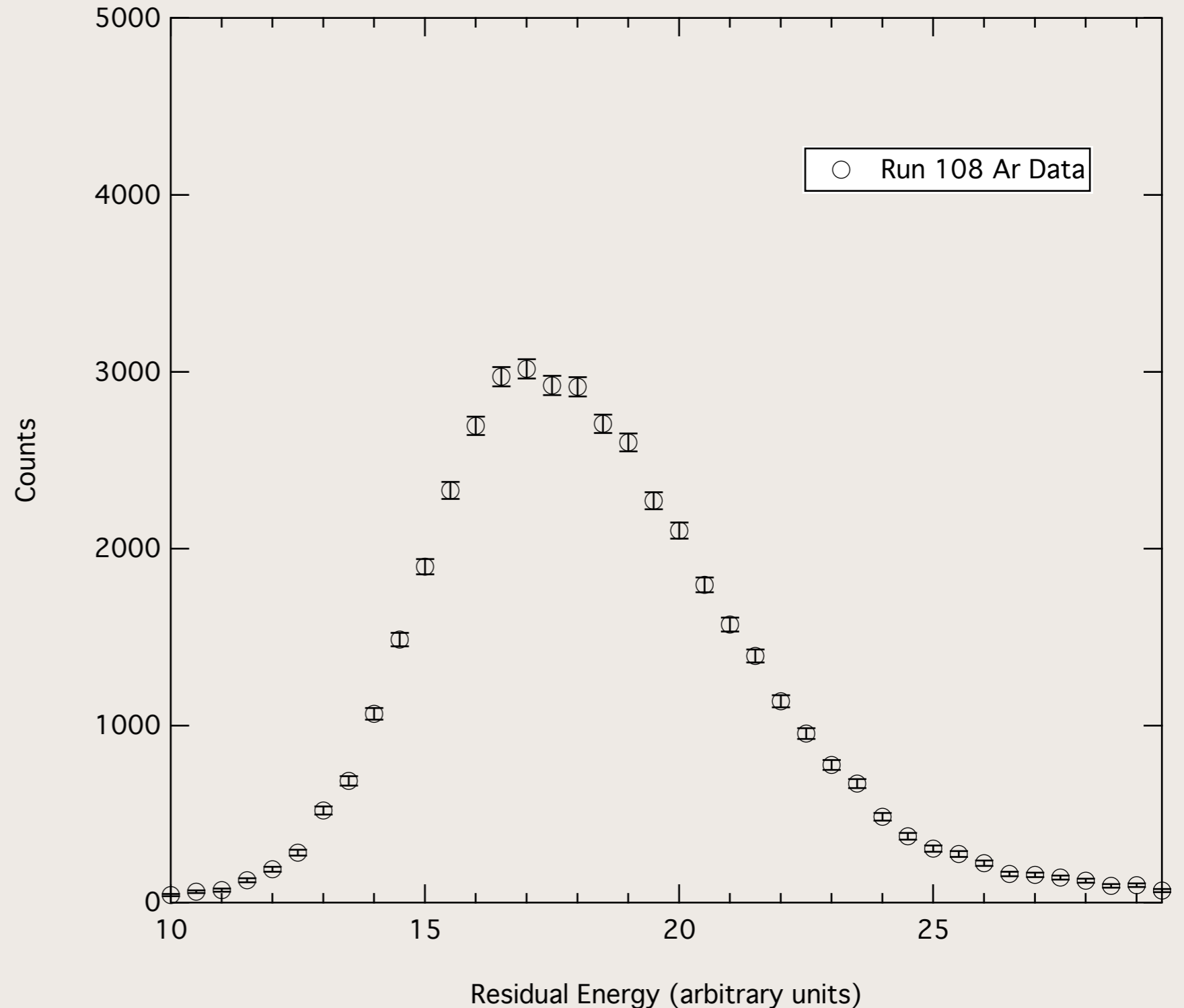
December 2016 Test: Ar

- There was no time to commission with an alpha source prior to December 16th beam time
- Bombarded thick Au foil with 80 MeV ^{36}Ar beam
- Tuned for multiply scattered beam with very large angular spread



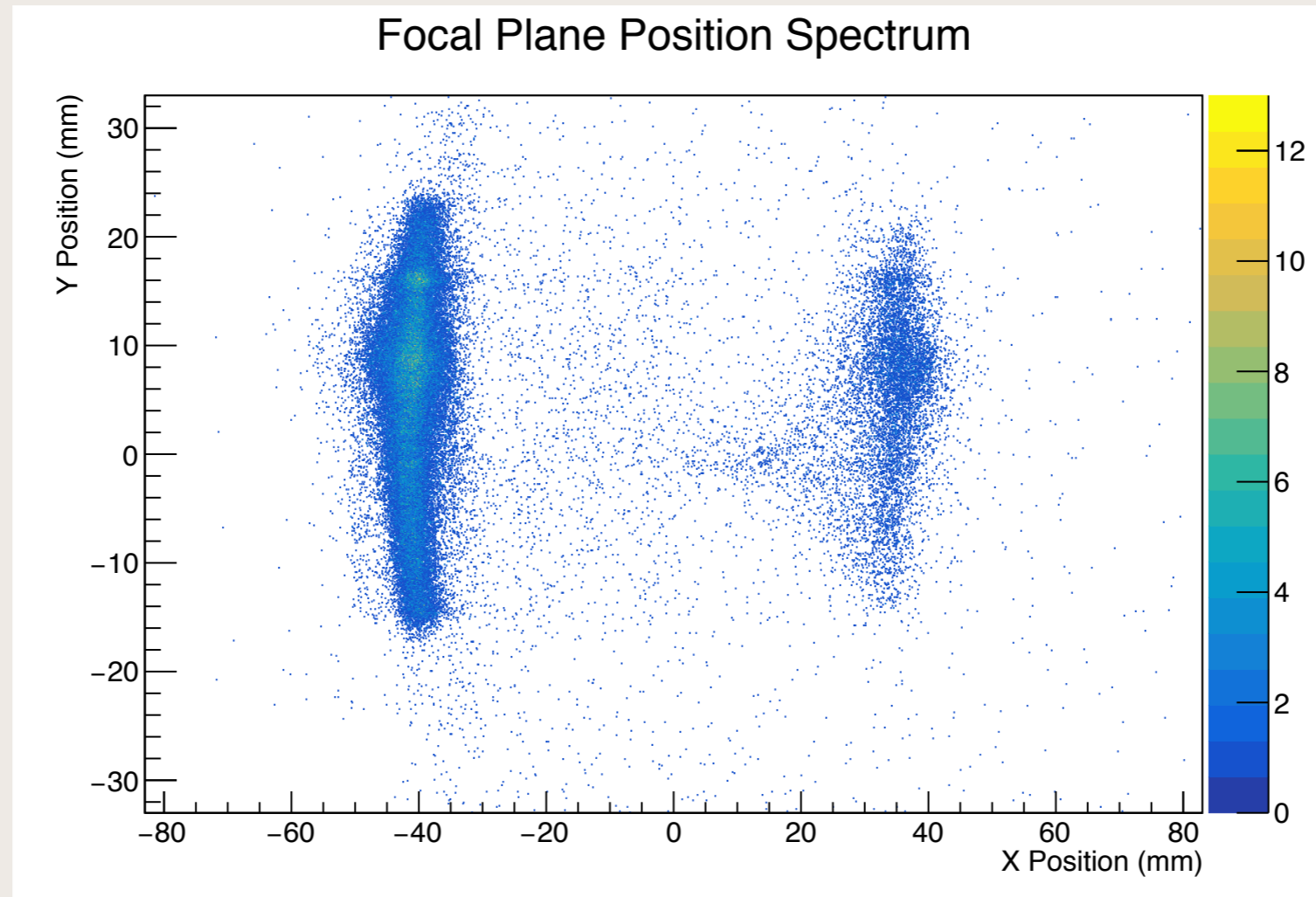
December 2016 Test: Ar

- Si-detector measured residual energy spread of 40% FWHM
- Consistent with filling nominal energy acceptance of +25%, -17%



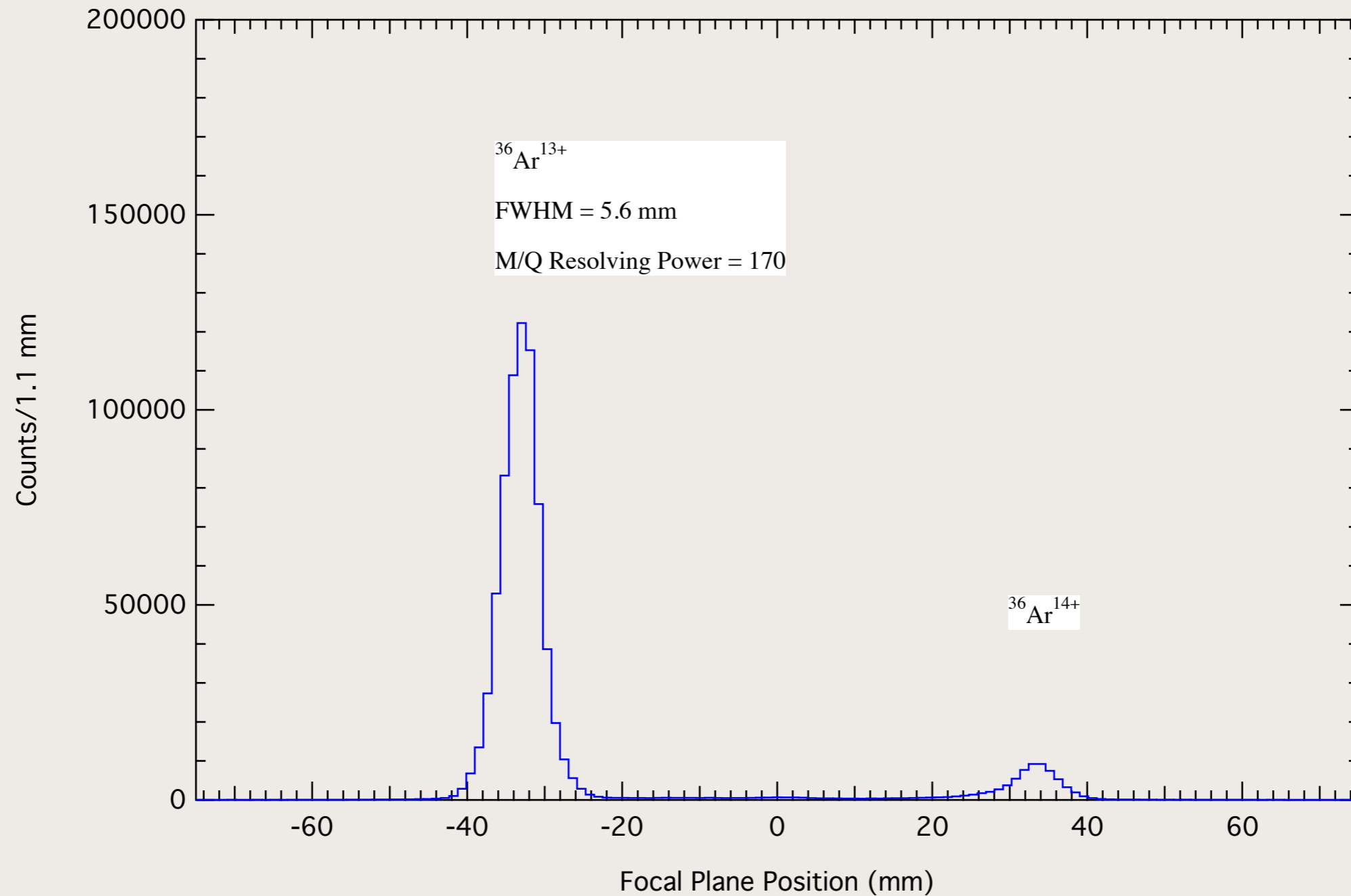
December 2016 Test: Ar

Measured Focal Plane Position Spectrum of Scattered ^{36}Ar



EMMA's First M/Q Spectrum

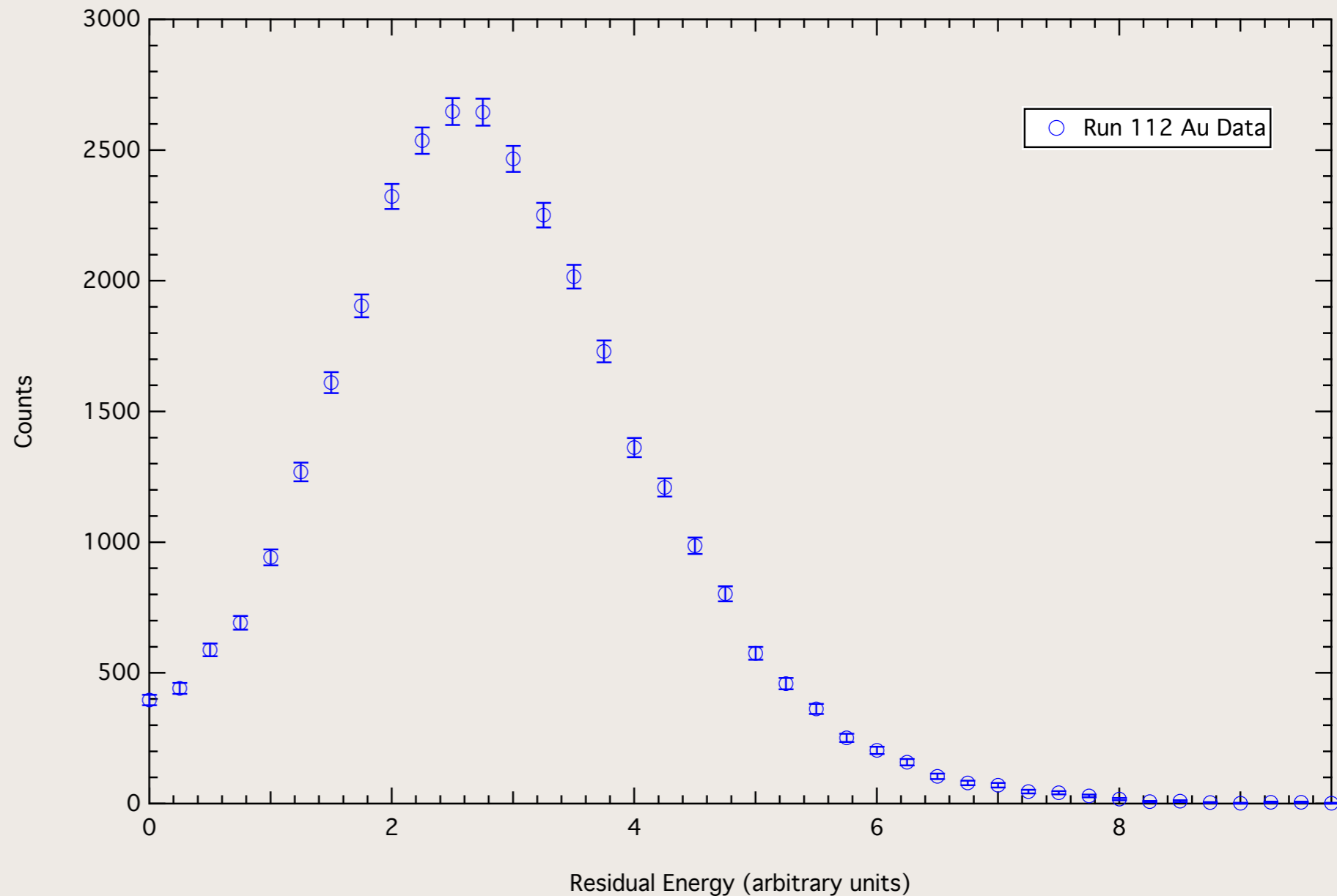
December 2016 Test: Ar



Measured mass/charge dispersion consistent with ion optical calculations

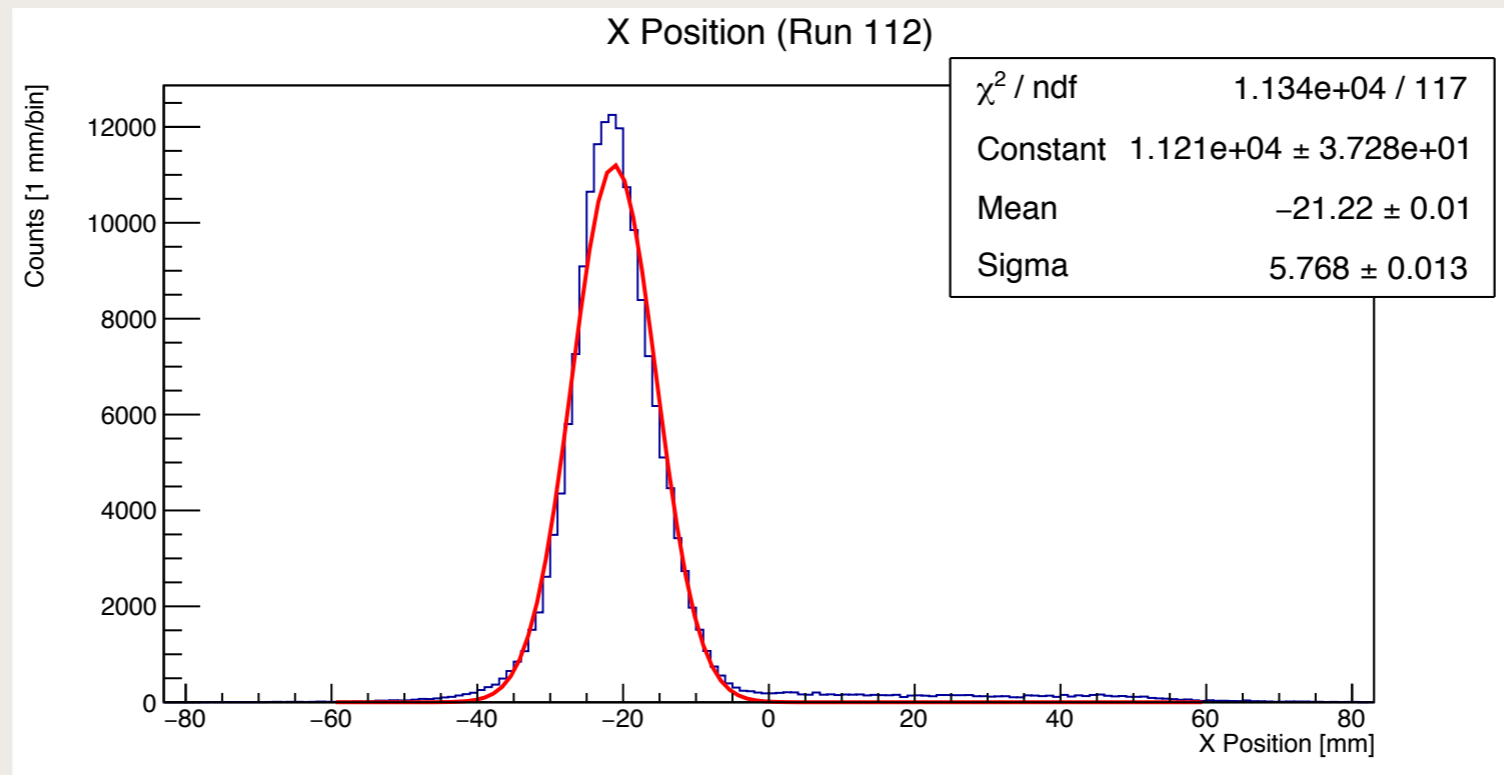
December 2016 Test: Au

- Si-detector measured residual energy spread of 111% FWHM
- Consistent with filling energy acceptance + energy loss straggling in PGAC windows



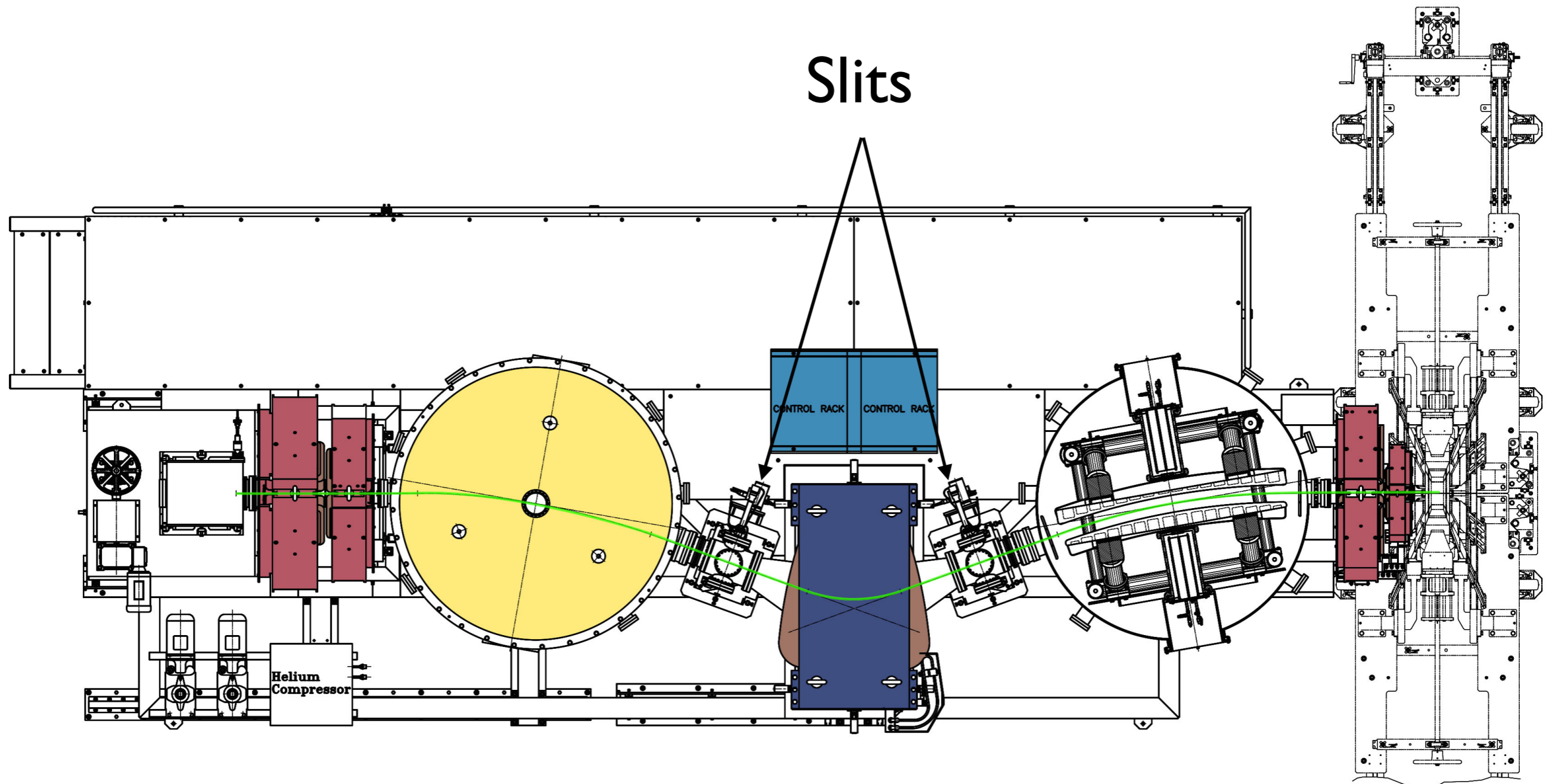
December 2016 Test: Au

Measured Focal Plane Position Spectrum of Scattered ^{197}Au

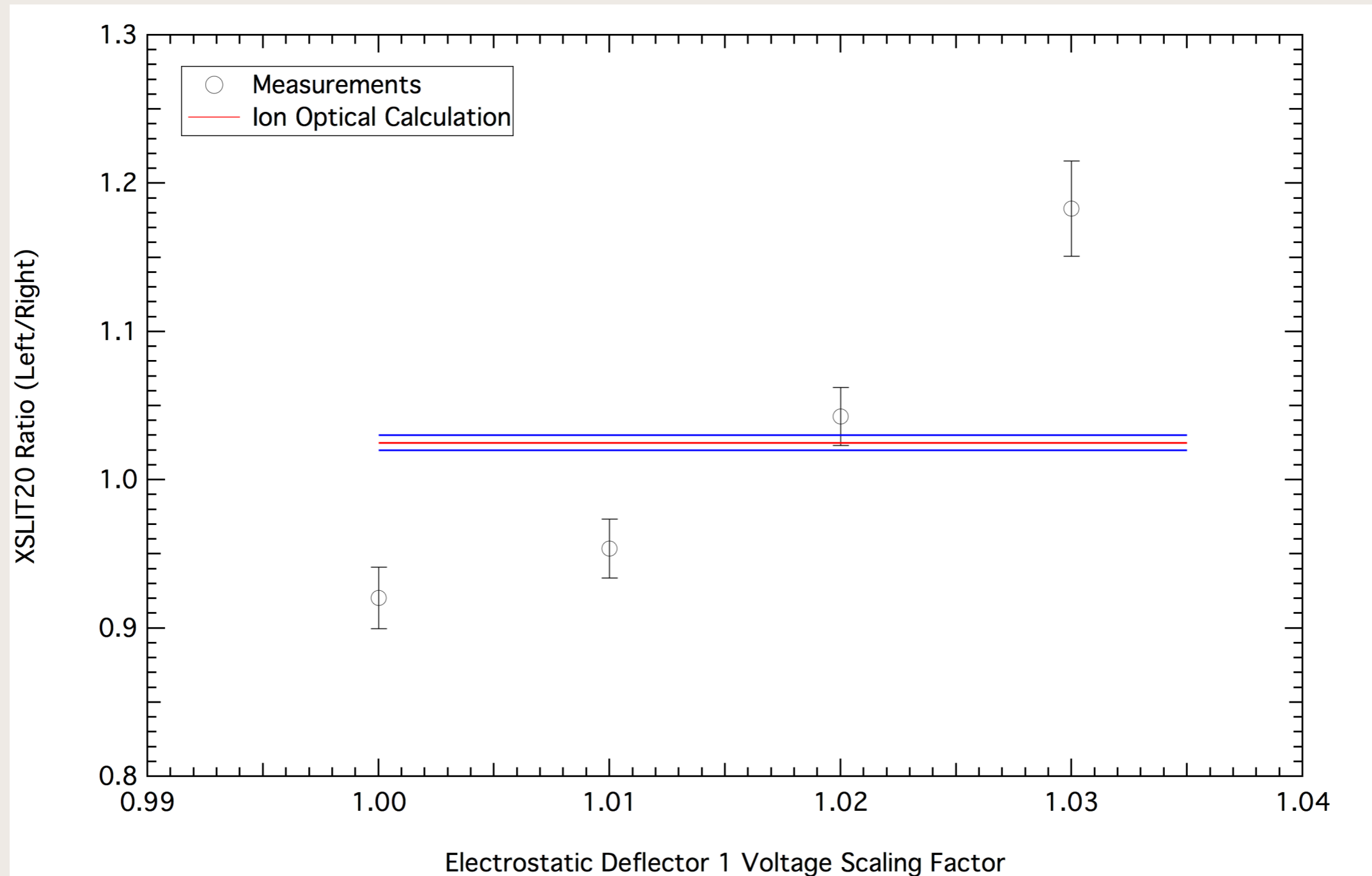


Set for $^{197}\text{Au}^{9+}$, observed single mass peak, little background in hour-long run with 10^9 ions/s on target

Transmission Studies with Slits



ED1 Voltage Variation



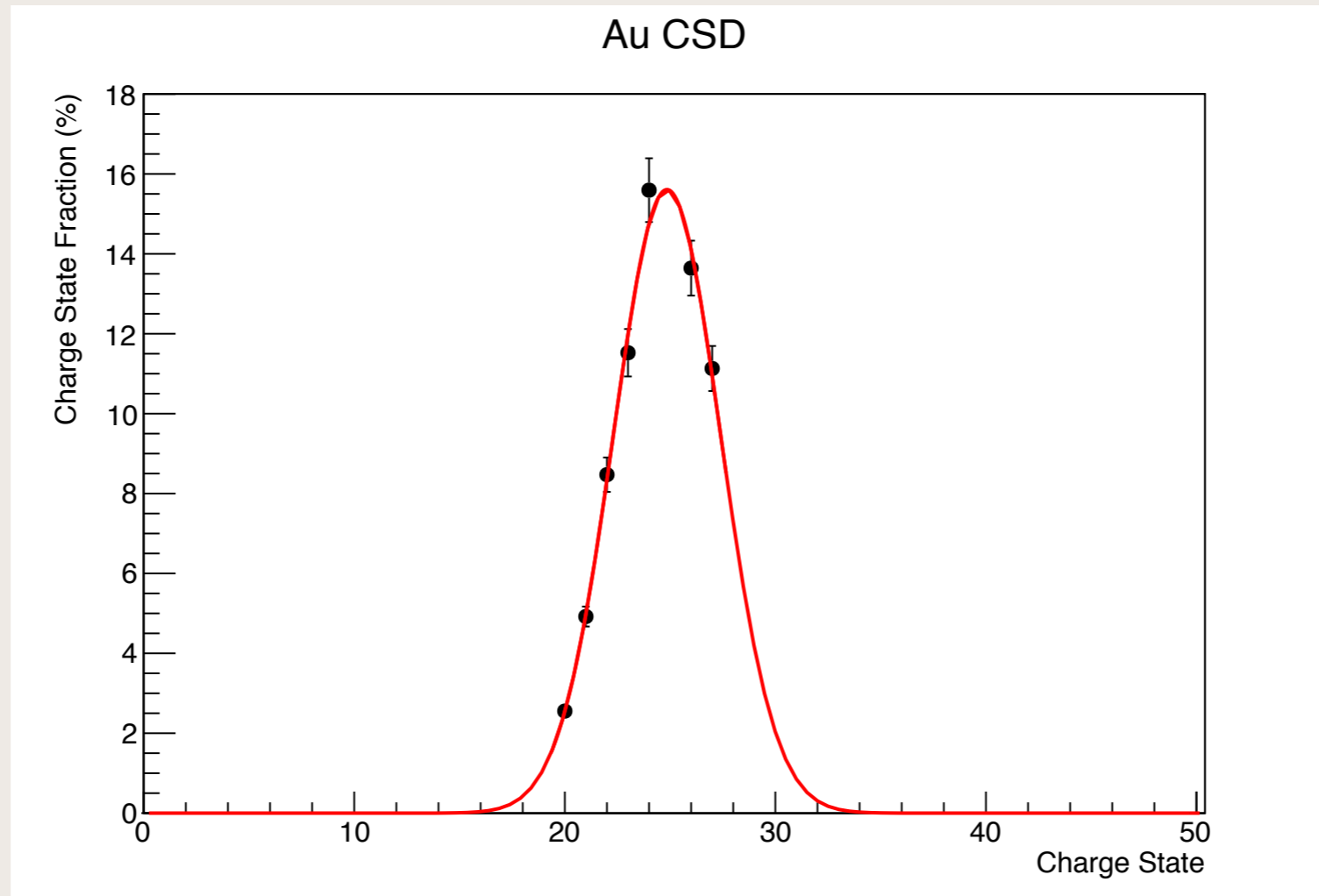
Acceptance Measurements

- Trajectories within spectrometer depend only upon angle and deviations of mass/charge and kinetic energy/charge with respect to central value
- Can mistune spectrometer in mass/charge to study mass/charge acceptance
- Mistune spectrometer in kinetic energy/charge to infer energy/charge acceptance
- Central value is irrelevant, so can use alpha source or elastic scattering to characterize

September 2017 Test Run

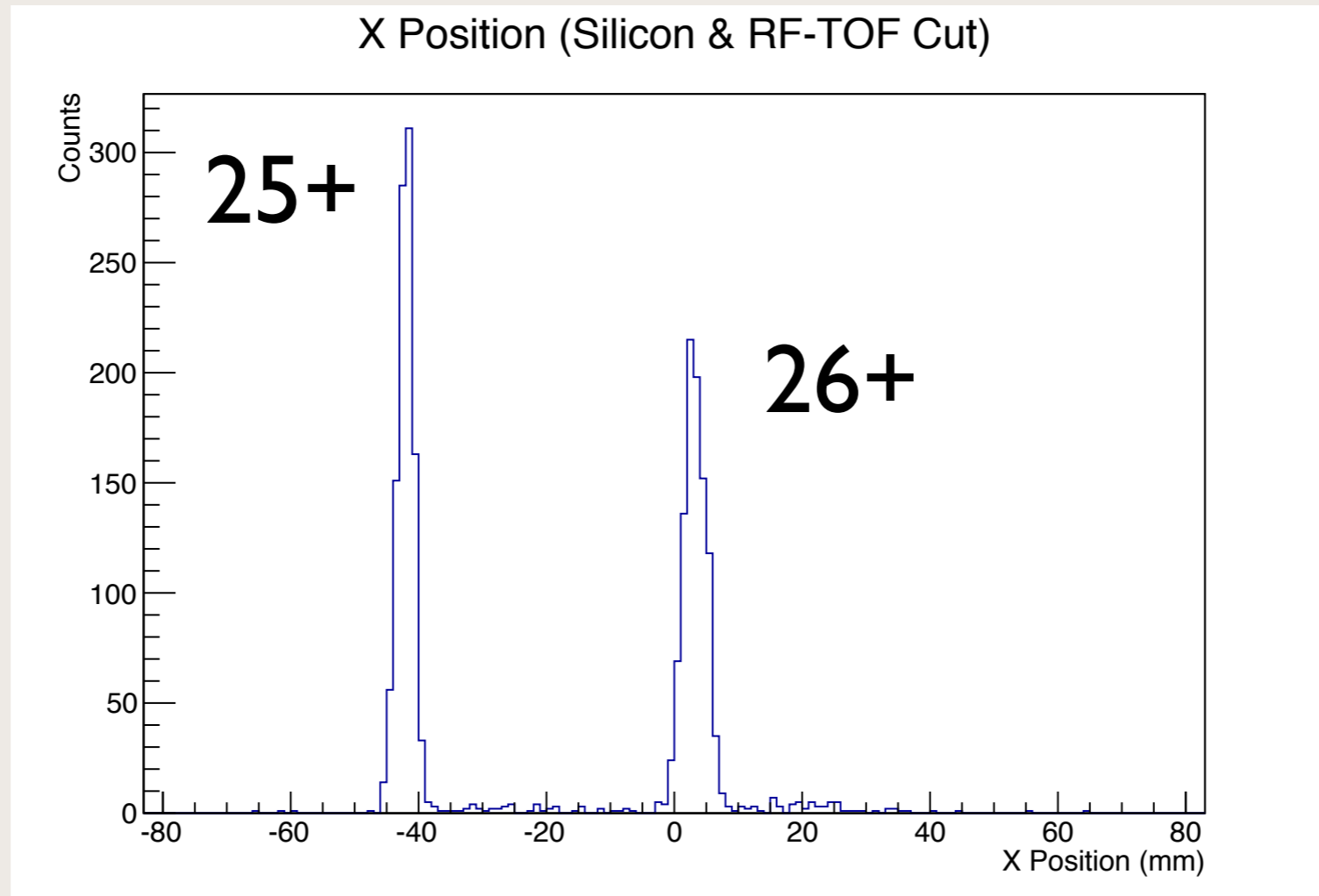
- Bombarded $50 \mu\text{g}/\text{cm}^2$ Au target with 120 MeV ^{40}Ar beam
- Set spectrometer for elastically backscattered 66 MeV ^{197}Au recoils in various charge states
- Excellent beam suppression
- Measured charge state distribution
- Used angular apertures in target chamber to define entrance angles, map out mass/charge and energy/charge acceptances
- Incident flux measured with SSBs in target chamber

Au Charge State Distribution



Gaussian fit integrates to 96(3)% of incident beam current

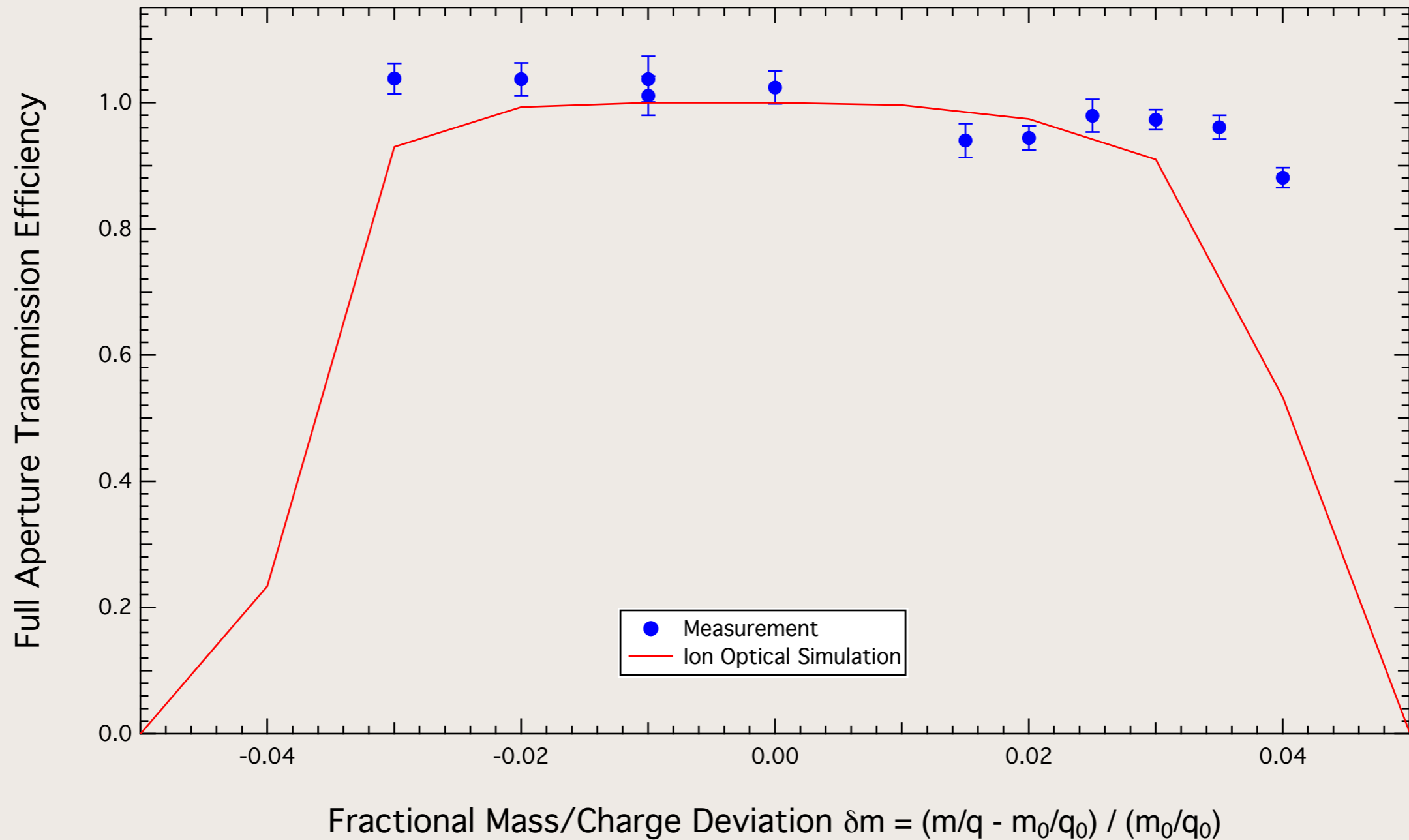
^{197}Au M/Q Spectrum



M/Q dispersion = 10 mm/%

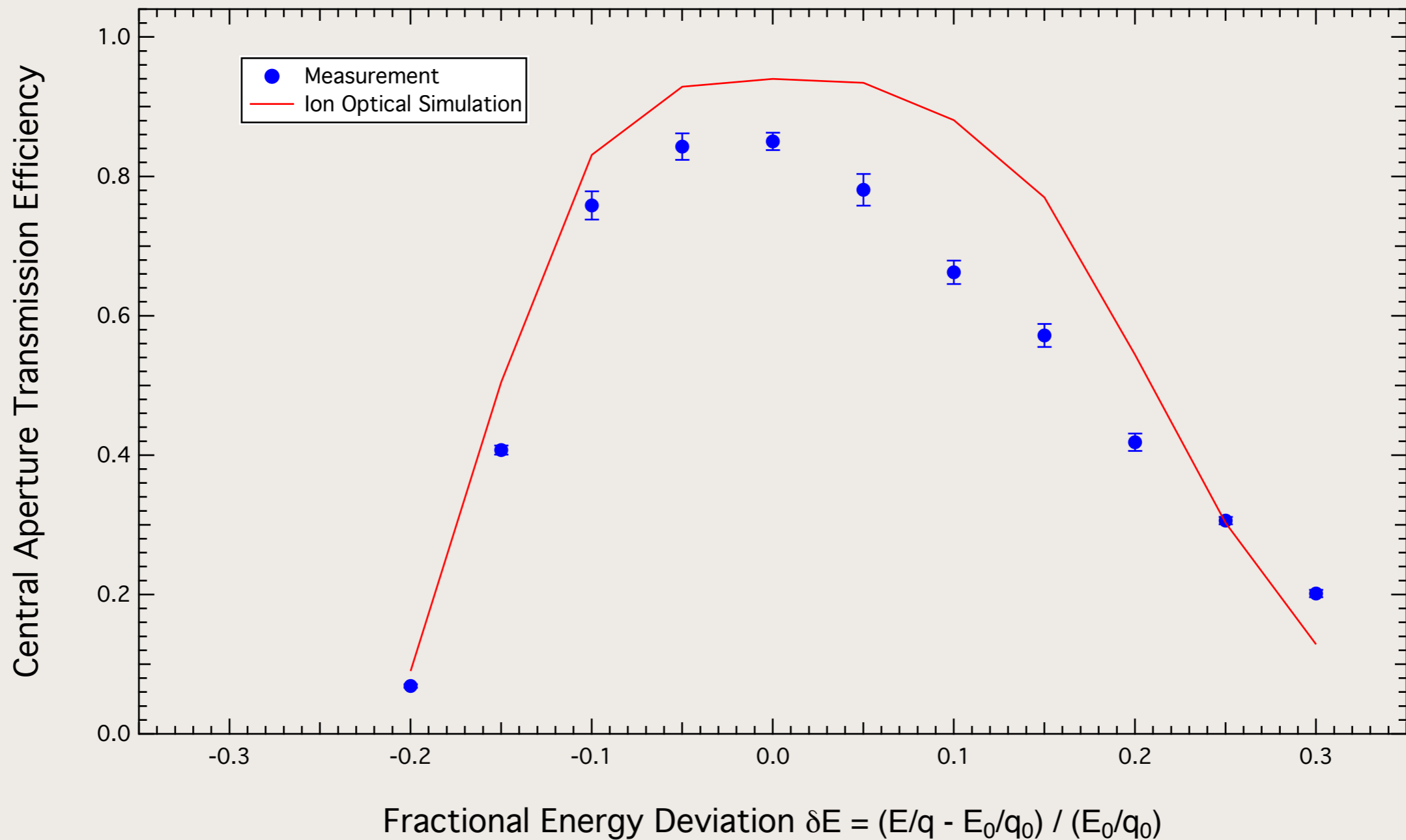
- Q = 25 peak has FWHM of 2.9 mm, implying resolving power of 340

M/Q Acceptance



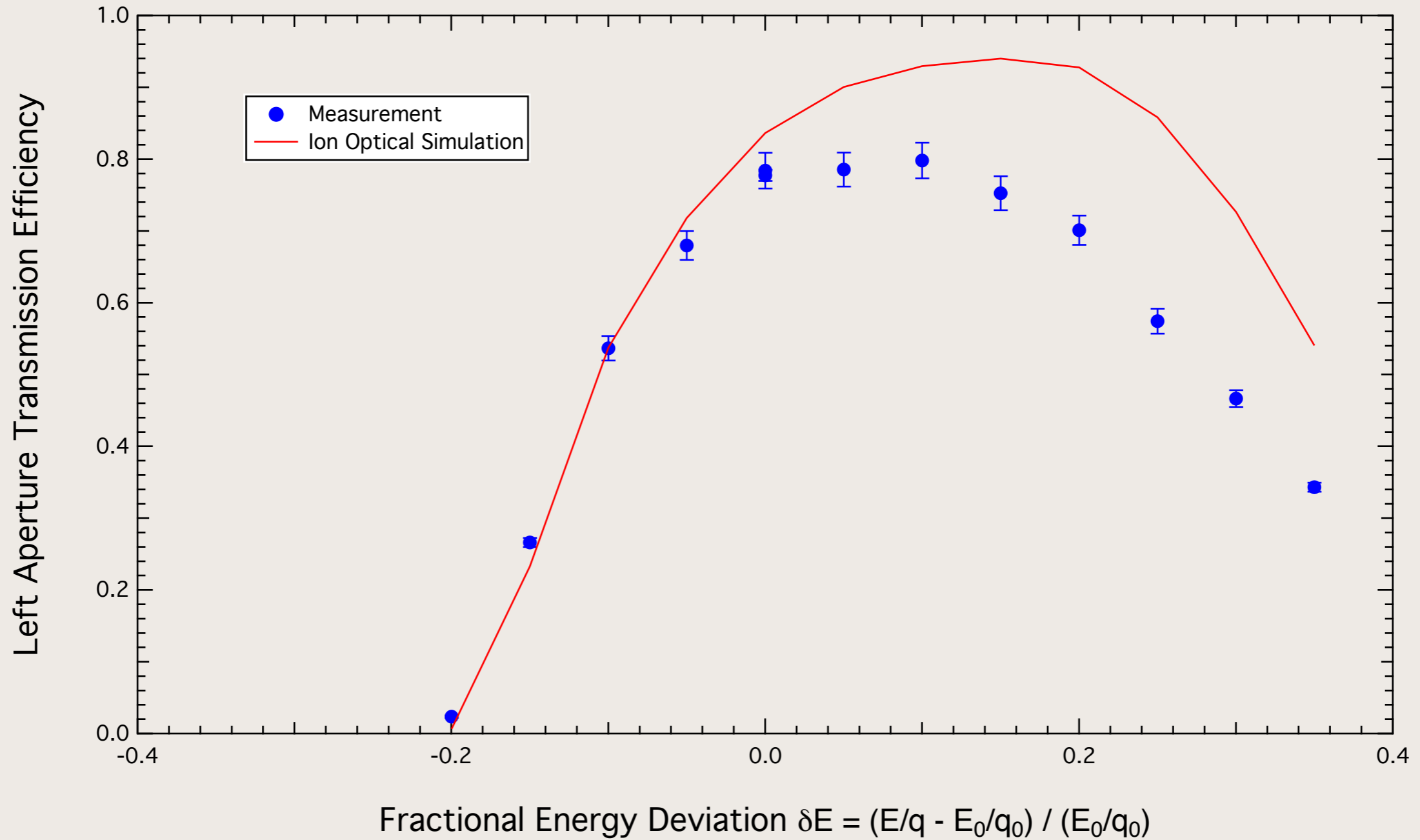
Full aperture: $\pm 3^\circ$ by $\pm 3^\circ$
 Consistent with $\pm 3.5\%$ m/q acceptance

E/Q Acceptance



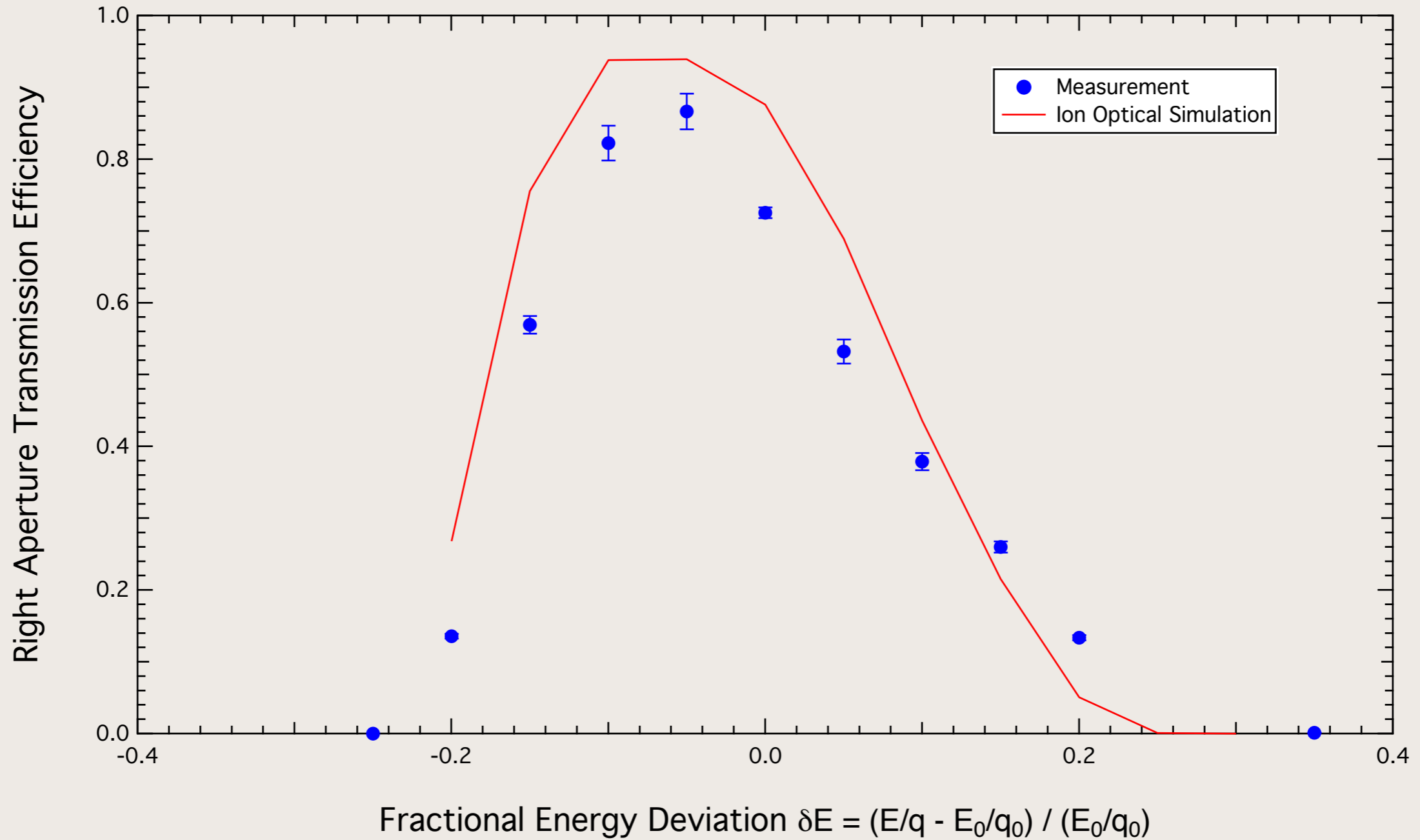
Measurements with ^{148}Gd source at target position with various angular apertures; here $\pm 1.2^\circ$ by $\pm 1.2^\circ$

Left Aperture



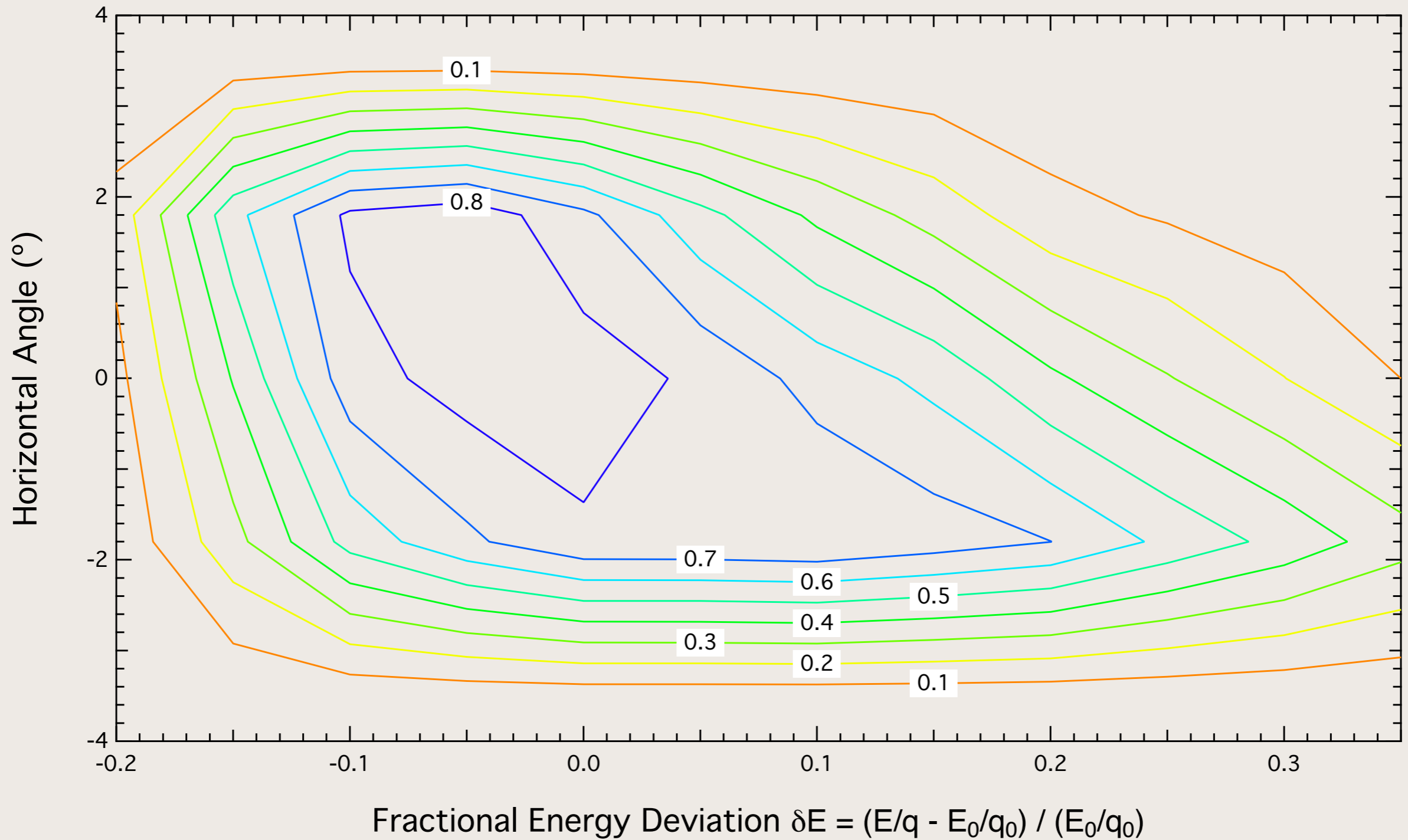
Left Aperture: -3° to -0.6° by $\pm 1.2^\circ$

Right Aperture

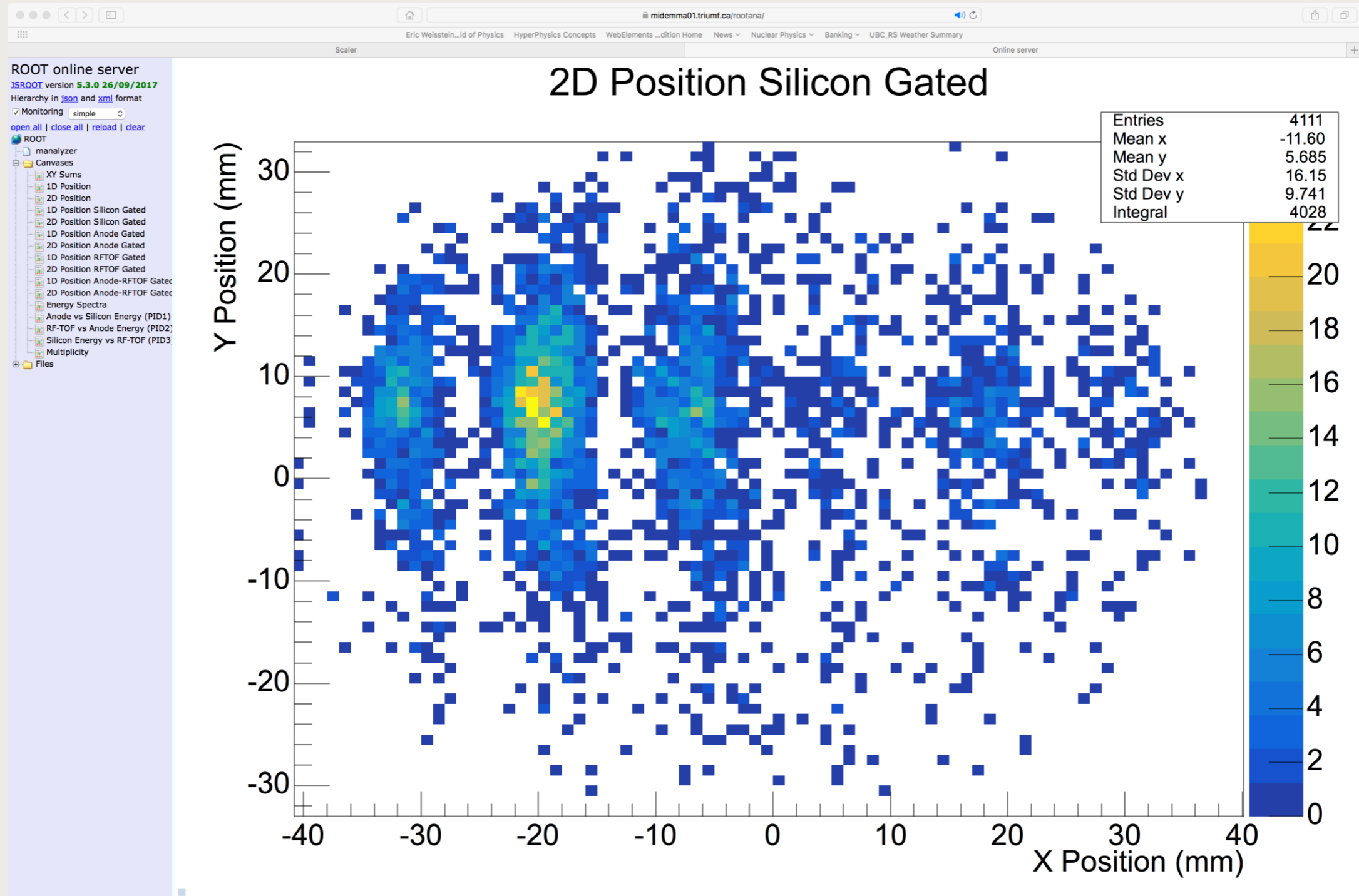


Right Aperture: 0.6° to 3° by $\pm 1.2^\circ$

2D Transmission Matrix

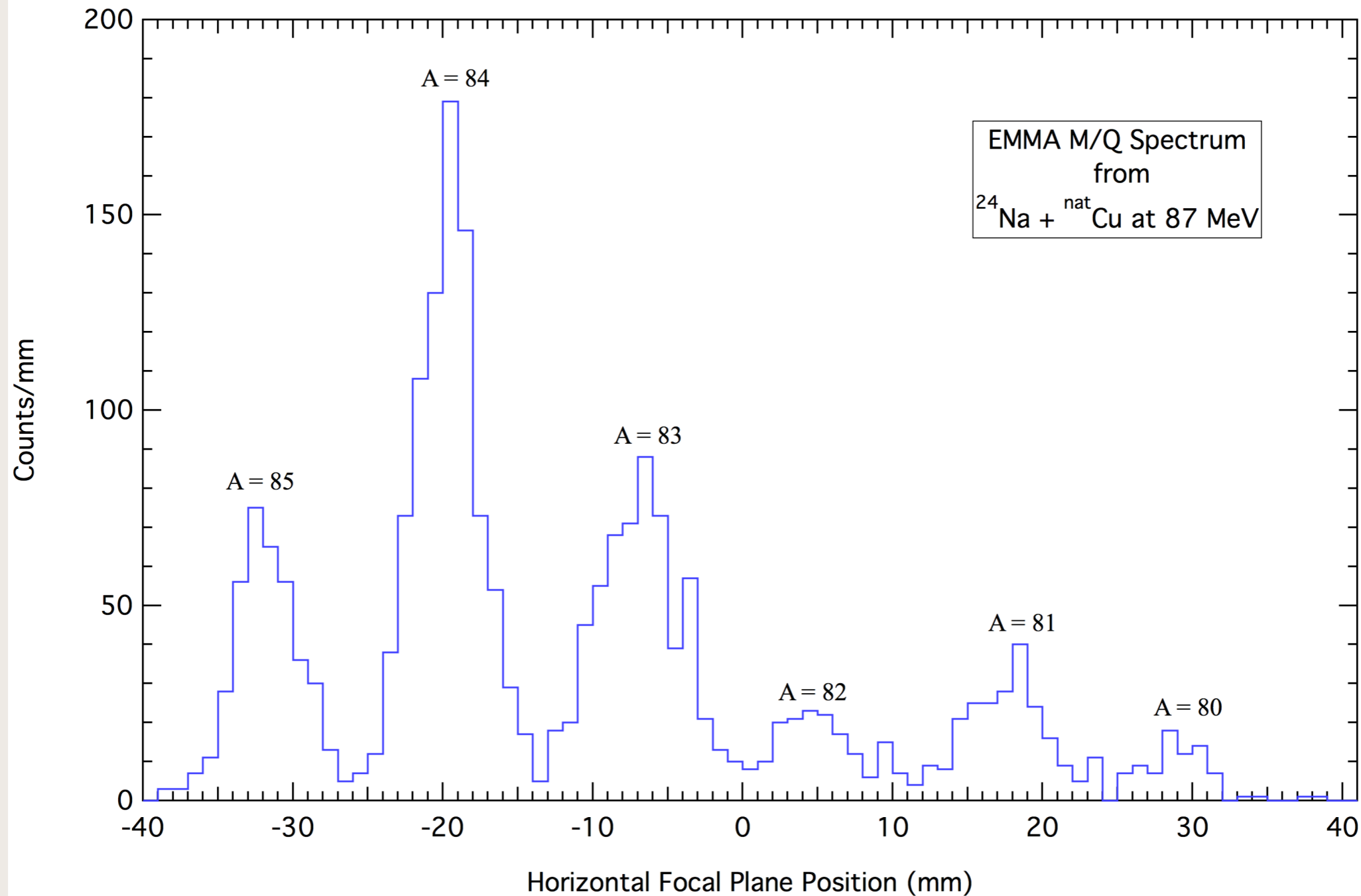


Fusion Evaporation with RIB



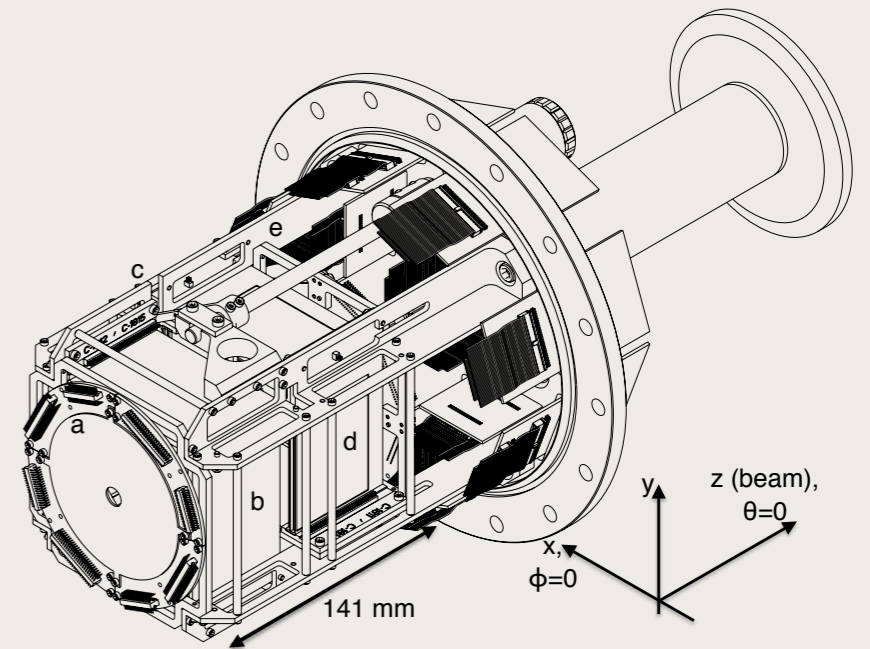
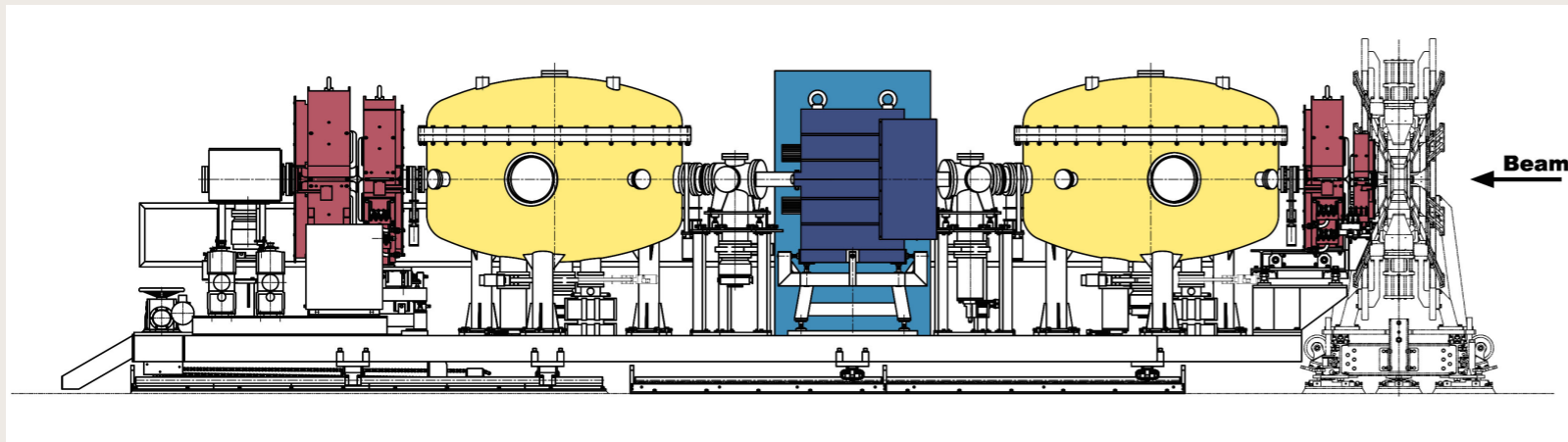
- Bombarded $890 \mu\text{g}/\text{cm}^2$ Cu target with ^{24}Na beam at 87 MeV
- Set spectrometer for fusion products with 17 MeV, $A = 82$, $q = 11$ ⁶⁰

Fusion M/Q Spectrum



- ^{24}Na beam intensity ranged from $1-4 \times 10^7 \text{ s}^{-1}$
- $q = 10$, full energy acceptance = 40% FWHM

Approved Experiments



- Four approved experiments, three of which require TIGRESS to be installed around EMMA target position
- Transfer experiments: ${}^6\text{Li}({}^{17}\text{O},\text{d}){}^{21}\text{Ne}$ to infer ${}^{17}\text{O}(\alpha,\gamma){}^{21}\text{Ne}$ reaction cross section for the s process; requires SHARC; ${}^{21}\text{Na},\text{Ne}(\text{d},\text{p})$ and (d,n) for isospin symmetry tests
- Radiative capture experiment: direct measurement of $\text{p}({}^{83}\text{Rb},\gamma){}^{84}\text{Sr}$ reaction cross section at p process energies
- $\text{p}({}^{21}\text{Na},\alpha){}^{18}\text{Ne}$ to infer ${}^{18}\text{Ne}(\alpha,\text{p}){}^{21}\text{Na}$ reaction cross section for Type I X-ray bursts
- Approved Letters of Intent: direct measurement of $\text{p}({}^{79}\text{Br},\gamma){}^{80}\text{Kr}$ reaction cross section and ${}^{34\text{m}}\text{Cl}(\text{d},\text{p})$ transfer for $\text{p}({}^{34\text{m}}\text{Cl},\gamma)$ in novae

Future Plans

- $^{20}\text{Ne}(p,\gamma)^{21}\text{Na}$ test June 25th
- Complete HV conditioning
- TIGRESS move to EMMMA target position
- (d,p) test in September
- First experiments in fall 2018 with TIGRESS

Core Personnel

- **Martin Alcorta, ISAC Target & Detector Physicist**
- **Franco Cifarelli, Mechanical Designer**
- **Nicholas Esker, Postdoctoral Researcher**
- **Kevan Hudson, MSc Student**
- **Naimat Khan, Project Engineer**
- **Peter Machule, Expert Technician**
- **Matt Williams, PhD Student**